



Effects of HIV gp120 on Neuroinflammation in Immunodeficient vs. Immunocompetent States

Taxiarhia J. Arabatzis^{1,2} · Alexa A. Wakley¹ · Virginia D. McLane^{1,3,4} · Dalton Canonico² · Ling Cao^{1,3} 

Received: 18 November 2019 / Accepted: 17 June 2020 / Published online: 6 July 2020
© Springer Science+Business Media, LLC, part of Springer Nature 2020

Abstract

HIV affects 37 million people worldwide, 25–69% of which develop HIV-associated neurocognitive disorders (HAND) regardless of antiviral treatment. HIV infection of the brain decreases cognitive function, disrupts/impairs learning and memory, and reduces quality of life for those affected. HIV-induced neuroinflammation has been associated with viral proteins such as gp120 and Tat, which remain elevated in the CNS even in patients with low peripheral viremia counts. In this study, we examined the effects of gp120 on neuroinflammation in immunodeficient vs. immunocompetent states by examining neuroinflammatory markers in gp120tg mice with or without systemic immunodeficiency caused by murine retroviral administration (LP-BM5 murine AIDS). Changes in inflammatory cytokine/chemokine mRNA expression was complex and dependent upon expression of gp120 protein, immunodeficiency status, brain region (hippocampus, frontal lobe, or striatum), and age. Gp120 expression reduced hippocampal synaptophysin expression but did not affect animals' learning/memory on the spontaneous T-maze test in our experimental conditions. Our results emphasize the critical role of the neuroinflammatory micro-environment and the peripheral immune system context in which gp120 acts. Multiple factors, particularly system-level differences in the immune response of different brain regions, need to be considered when developing treatment for HAND.

Keywords gp120 · LP-BM5 · Neuroinflammation · HAND · Hippocampus · T-maze

Introduction

Nearly 37 million people throughout the globe are infected with human immunodeficiency virus-1 (HIV-1) (https://www.unaids.org/sites/default/files/media_asset/AIDS-by-the-numbers-2016_en.pdf), with 1.1 million of those infected living in the US (Force 2019). Current major risk factors for contracting HIV in the US include men who have sex with

men (67% of new cases), as well as intravenous drug abuse (4% of new cases in men and 12% of new cases in women) (Force 2019). Modern antiretroviral drug treatment regimens can significantly reduce viral load. However, access to care, consistency of treatment, and management of side effects remain insufficient, especially for populations with low compliance or delayed treatment (Maartens et al. 2014). According to the CDC, within the US, only 30% of HIV patients have viral loads that are controlled by antiretroviral therapy (Bradley et al. 2014). Further, when the CSF of patients with suppressed plasma HIV RNA and adequate CD4 levels was examined, nearly 50% of the participants still had detectable HIV-infected cells (Spudich et al. 2019). HIV proteins were also detected in spinal fluid despite low peripheral viremia counts achieved through antiretroviral therapy (Henderson et al. 2019). Thus peripheral viral suppression does not reflect the CNS viral status.

Chronic complications associated with HIV/AIDS are becoming more prevalent as patients with HIV continue to live longer (Watkins and Treisman 2015). HIV-associated neurocognitive disorders (HAND) affect 25–69% of individuals with HIV, with variation in the presentation and severity

✉ Ling Cao
lcao@une.edu

¹ Department of Biomedical Sciences, University of New England College of Osteopathic Medicine, 11 Hills Beach Road, Biddeford, ME 04005, USA

² Department of Biology, University of New England College of Arts and Sciences, Biddeford, ME, USA

³ Graduate School of Biomedical Science and Engineering, University of Maine, Orono, ME, USA

⁴ Present address: Department of Pharmacology and Toxicology, Virginia Commonwealth University, Medical College of Virginia (MCV) Campus, P.O. Box 980613, Richmond, VA 23298-0613, USA

of symptoms (Letendre et al. 2009). HIV infection of the brain decreases cognitive function, affects memory and learning, reduces the ability to carry out everyday tasks, maintain employment, and negatively impacts the overall quality of life (Letendre et al. 2009). Clinical manifestations of HAND can be asymptomatic, mild, or severe HIV-associated dementia (HAD) (Nasi et al. 2017). The symptoms and severity of HAND are also dependent on infection progression, antiviral treatment, age, and other factors such as the use of opioid drugs (prescription or illicit use) (Anthony et al. 2005, 2008; Bell 2004; Bell et al. 1998; Hauser and Knapp 2014; Letendre et al. 2009; Weisberg et al. 2015). A 2019 study reported a significant association between the detection of cell-associated HIV DNA and poor neurocognitive function (Spudich et al. 2019). Although diagnosis of HAD has decreased in recent years, the prevalence of asymptomatic and mild forms of HAND has not. As a result, patients are vulnerable to the development of more severe symptoms as they age (Dickens et al. 2017; Janssen et al. 2015; Piggott et al. 2020; Saylor et al. 2016). Therefore, it is critical to treat HAND promptly, while developing new therapies to combat the effects of HAND, as currently there are no FDA-approved treatments directly targeting HAND (Letendre et al. 2009; McArthur et al. 2010; Nasi et al. 2017).

The development of HAND is believed to be the result of both direct and indirect damage caused by the virus. Inflammatory HIV proteins (e.g., HIV-Tat, gp120) released in the brain could contribute to the damage seen within the striatum, hippocampus, and to some extent the frontal lobe, regions known to be responsible for executive functions, attention, memory, and learning (Ellis et al. 2007). HIV-associated CNS pathology involves synaptodendritic neuronal injury, resulting in abnormal neuronal connectivity and subsequent deficits in cognitive skills and behavior (Ellis et al. 2007; Masliah et al. 1997; McLaurin et al. 2019; Moore et al. 2006). The neuronal damage observed in patients with HAND is primarily associated with persistent inflammation in the CNS (McArthur et al. 2010; Nasi et al. 2017; Saylor et al. 2016). Several cytokines that contribute to the activation of macrophages, microglia, and astrocytes as well as help promoting further neuroinflammation are found to be upregulated or dysregulated in the CNS of patients with HIV/AIDS, including: monocyte chemoattractant protein-1 (MCP-1, also known as CCL2), regulated upon activation normal T cell expressed and secreted (RANTES, also known as CCL5), macrophage inflammatory protein-1 alpha (MIP-1 α , also known as CCL3), macrophage inflammatory protein-1 beta (MIP-1 β , also known as CCL4), interferon gamma-induced protein-10 (IP-10/CXCL10), tumor necrosis factor (TNF- α), interleukin-12 (IL-12), and interleukin 8 (IL-8), as well as antiviral interferons (IFNs) interferon alpha (IFN α), interferon beta (IFN β), and interferon gamma (IFN γ) (Brabers and Nottet 2006; Cary et al. 2013; Deshmane et al. 2009; Gonzalez et al. 2002; Kelder et al. 1998; Kolb et al. 1999; Sirovica et al. 2014; Watanabe et al. 2010).

These observations support the idea that a strong milieu of inflammatory mediators are constantly released in the CNS of HIV patients and are likely contributing to CNS damage and the pathophysiology of HAND.

HIV is a distinctly neurotropic and neurovirulent retrovirus that can enter the CNS within weeks of infection via diapedesis of infected peripheral CD14+CD16+ monocytes across the blood-brain barrier (Williams et al. 2014). Several HIV proteins including gp120 have been shown to contribute to the neuropathology of HAND. Gp120 has been found to induce neurotoxicity through damaging neuronal mitochondria in patients infected with HIV (Avdoshina et al. 2016; Fields et al. 2016), via the p38 MAPK pathway (Zhu et al. 2015) and by inducing intracellular calcium dysregulation (Haughey and Mattson 2002), all of which could lead to memory deficits and the pathogenesis of HAND. Gp120-induced neurotoxicity could be mediated in part by gp120-induced inflammation as gp120 was shown to increase TNF α , IL-1 β and IL-6 expression in primary brain microglia and astrocytes (Ronaldson and Bendayan 2006; Yeung et al. 1995). Gp120tg mice were also found to display upregulated levels of CXCL10 and CCL2 in the CNS (Asensio et al. 2001). In addition, blocking the NF- κ B pathway resulted in reduced pro-inflammatory responses and enhanced neuroprotective effects of cultured astrocytes treated with gp120, highlighting the role of inflammation in gp120 induced neuronal damage (Janda et al. 2011). However, our knowledge regarding gp120's contribution to HAND pathology via neuroinflammation is still incomplete.

Due to the fact that HIV establishes itself within the CNS early in infection, and not all HIV-infected individuals have controlled peripheral viral loads and CD4 counts (in fact only 30% of HIV-infected individuals do (Bradley et al. 2014)), understanding the effects of neurotoxic HIV proteins such as gp120 on neuroinflammation in immunodeficient (with potential active viral replication) vs. immunocompetent states is critical and will allow us to further delineate the role of HIV proteins in HAND. The current study used HIV gp120tg mice, which constitutively express gp120 under a glial fibrillary acidic protein (GFAP) promoter, and share many distinctive changes found in the CNS of patients with HAND (Krucker et al. 1998; Thaney et al. 2017, 2018; Toggas et al. 1994), to examine the effects of gp120 on: 1) the expression of various neuroinflammation-related factors in hippocampus, striatum, and frontal lobe quantified via qRT-PCR, 2) hippocampal synaptophysin and microtubule-associated protein 2 (MAP2) expression measured by ELISA, and 3) learning/memory function assessed through the spontaneous T-maze. To induce an immunodeficient state, gp120tg mice were infected with LP-BM5, a murine retroviral mixture known to cause immunodeficiency (referred to as murine AIDS or MAIDS in previous studies) (Green et al. 2013; Li and Green 2006; Mutnal et al. 2013).

Material and Method

Mice

All mice were housed at the University of New England (UNE) animal facility and were provided food and water ad libitum and kept on a 12-h light/dark cycle. B6.SJL gp120tg mice (referred to as gp120tg mice in the text) were a gift from Dr. Marcus Kaul, Sanford Burnham Prebys Medical Discovery Institute, La Jolla, CA, USA. Gp120tg breeding was established within the UNE animal facility. HAND-like pathology significantly increases with age in gp120tg+ mice: physiological and morphological changes were detected at 3–5 months of age, while behavioral changes were detected around 7–9 months of age (D'Hooge et al. 1999; Maung et al. 2014; Toggas et al. 1994). As the effects of immunodeficiency in this model were unknown, both young (8–10 weeks old) and old (~5 months old) gp120tg mice were included in the study. Gp120tg mice were maintained through heterozygous breeding. Littermate gp120tg- were used as controls to examine the effects of gp120 expression. Both male and female mice were used in each group. At twelve weeks post-infection mice were sacrificed via CO₂ inhalation following T-maze assay (See below), i.e. mice were about 4–5 months and 7–8 months old respectively at sample collection. Blood was collected via cardiac puncture and tissues were then harvested, snap frozen on dry ice, and stored at –80 °C until further analysis. Twelve weeks of infection was chosen based on our previous studies with the susceptible C57BL/6 mice (Cao et al. 2012), in which viral loads in the peripheral tissues started to plateau between 2 and 6 weeks post-infection depending on the tissues examined. Serum Ig levels started to plateau around 8 weeks post-infection. Spleen weight continued to increase up to 12 weeks post-infection (when the experiment was terminated). Animals followed up to 12 weeks post-infection did not show obvious sickness behaviors except that their body weight was slightly greater than that of non-infected mice due to enlarged lymphoid tissues overtime. Thus, at 12 weeks post infection, immunodeficiency has fully developed without fatal outcomes being detected, therefore a 12-week time point was chosen in our current study. All experiments were approved by the Institutional Animal Care and Use Committee (IACUC) at the UNE (Biddeford, ME) and were in compliance with the Animal Welfare Act and NIH Guide for the Care and Use of Laboratory Animals (https://www.ncbi.nlm.nih.gov/books/NBK54050/pdf/Bookshelf_NBK54050.pdf).

LP-BM5 Virus Stock

LP-BM5 viral stock was derived from a complete LP-BM5 isolate stock provided by Dr. William Green (Dartmouth College Geisel School of Medicine, Hanover, NH). The stock

was maintained in our laboratory and viral load was titered by plaque assay as described previously (Cao et al. 2012). On day 0, mice were given 5×10^4 plaque-forming units (pfu) of the LP-BM5 retroviral mixture via intraperitoneal (i.p) injection. This viral dose was previously found to induce immunodeficiency, peripheral neuropathy, and CNS infection in C57BL/6 mice (Cao et al. 2012; Li and Green 2006; McLane et al. 2014, 2018). Non-infected mice did not receive an injection.

Evaluation of the Development of Systemic Immunodeficiency

Splenomegaly and hypergammaglobulinemia were used as measures of systemic immunodeficiency development (Li and Green 2006). Upon sacrifice of animals, spleens were collected, weighed, and frozen at –80 °C before RNA isolation. Serum was collected from the whole blood after clotting, and stored at –20 °C until further analysis. Spleen weight/body weight ratio was used to measure the development of splenomegaly to control for variation in individual mouse body weight. Serum immunoglobulin levels of IgG2a and IgM were assessed through enzyme-linked immunosorbent assays (ELISAs) (Cao et al. 2012; Li and Green 2006).

RNA Isolation and Quantitative Real Time Polymerase Chain Reaction (qRT-PCR)

RNA was isolated from the different brain regions (left side) and the spleen using RNeasy Lipid Tissue Kit (Qiagen, Waltham, MA) following the manufacturer's instructions. RNA (1 µg) was reverse-transcribed to 20 µl complimentary DNA (cDNA) using Quanta qScript Supermix (Quanta Bio, Beverly, MA). For qRT-PCR, 0.5 µl of cDNA was amplified with appropriate primer sets and Quanta PerfeCTa™ SYBR Green FastMix ROX (Quanta Bio, Beverly, MA) using an Applied Biosystems StepOnePlus Real-Time PCR thermocycler (Applied Biosystems, Forest City, CA). Viral RNA gene expression was measured using primers for BM5eco and BM5def gag genes and normalized to β-actin. Gp120 expression was measured using primers provided by Kaul lab and was normalized to GAPDH (University of California Riverside; personal communication). Cytokine/chemokine, CD11b, GFAP, synaptophysin, and MAP-2 RNA expression was measured using primers summarized in Table 1 and were normalized to GAPDH (Cao et al. 2012; Cook et al. 2003) (Integrated DNA Technologies, Inc., IDT, Coralville, IA). All primer sequences and qRT-PCR run methods are shown in Table 1. Expression for all markers was analyzed using the ΔΔCt method. All primers were synthesized by IDT. While PCR was run for both BM5def and BM5eco RNA in all tissues collected, expression levels were altered in similar ways by treatment. Only the

each test. In the first trial, the mouse was placed at the base of the maze (the bottom of the “T”) facing forward, with a central partition separating the sides of the T from each other and allowed to choose an arm. Following 30 sec of containment in the arm chosen by the mouse, the mouse was placed back into the beginning of the maze for the 0 min trial interval, or in a separate holding cage (not the home cage) for the 2 min trial interval, and the central partition was removed. For the second trial, the mouse was placed at the base of the maze and allowed to choose a side again. A “correct” response was recorded when the mouse chose the opposite arm in trial 2 compared to the one chosen in trial 1. An “incorrect” response occurred when the mouse chose the same arm in both trials. All animal testing was performed during the light period of the light-dark cycle. Mice were tested in two-three sessions (separated by 3–4 h) per day for 3–4 consecutive days. Within each session, each mouse was tested once for each retention interval, with at least 30 min in between the two tests. Each mouse received a total of 8–9 tests with each retention interval. The percentage of correct responses was calculated for each mouse and each retention time to represent each mouse’s working memory. During trial 1 of each test, “time to choice” was also recorded to determine whether there was motivational or motor function related delay that affected animals’ ability to choose an arm.

Statistical Analysis

Data were analyzed and graphed using SigmaPlot/SigmaStat 10 software (Systat Software Inc., San Jose, CA). Sex differences were not detected in our initial analysis of all data collected, thus data obtained from males and females were combined in final data analysis. Outlier analysis was performed using the Grubbs Test through the GraphPad online resources, QuickCalcs (<https://www.graphpad.com/quickcalcs/Grubbs1.cfm>) (GraphPad Software Inc., La Jolla, CA). Data (except Figs. 2, 9 and 10) were graphed in the format of interaction plots and analyzed using two-way analysis of equal variance (ANOVA) using LP-BM5 treatment (2 levels) and group (4 levels; classified based on animals’ age and genotype) as between subject factors followed by the Tukey post hoc test. When a main effect from at least one factor was found but an interaction was not detected, simple effects analyses (i.e., analysis of the differences in the mean treatment responses for one factor was conducted separately for each level of the other factor) were examined as necessary to decipher individual treatment group differences as described previously (Wei et al. 2012). In some instances, data were log-transformed in order to obtain data sets with normal distribution before ANOVA analysis. Figure legends are annotated where applicable. For T maze data

(Fig. 10), Wilcoxon Signed Rank Test was used to determine the overall differences between 0 vs. 2 min intervals first, then within each interval, data were graphed and analyzed via two-way ANOVA followed by Tukey *post-hoc* test as described above. For viral load data (Fig. 2), BM5Def was not detectable in group that was not treated with LP-BM5 and data sets did not have normal distribution. Therefore, these data sets were analyzed using Kruskal-Wallis One-way ANOVA on Ranks followed by the Dunn’s *post-hoc* test was performed with log-transformed values. For the ELISA on synaptophysin (Fig. 9), three-way ANOVA with gp120, age and LP-BM5 as factors was performed followed by the Tukey post hoc test. All data are presented as mean \pm SEM, with $p \leq 0.05$ considered to be statistically significant.

Results

Development of Immunodeficiency in gp120tg Mice Treated with LP-BM5

C57BL/6 mice are the susceptible mouse strain for LP-BM5 (Hartley et al. 1989; Huang et al. 1992). Because gp120tg mice have C57BL/6 and SJL mixed background, first we tested whether immunodeficiency can be established in gp120tg mice. Typically, LP-BM5-induced immunodeficiency is indicated by splenomegaly (Fig. 1a), and hyperimmunoglobulinemia (Fig. 1b and c), along with the detection of viral gag RNA in the spleen (BM5Def, Fig. 2a) (Li and Green 2006). For spleen/body weight ratio, serum IgM and IgG2a, a significant main effect of LP-BM5 treatment was detected regardless of gp120 expression or age of the animals (Two-way ANOVA (log-transformed data for all): Fig. 1a, spleen/body weight ratio, $p_{LP-BM5} < 0.001$, $p_{group} = 0.542$, $p_{LP-BM5 \times group} = 0.510$; Fig. 1b, serum IgM, $p_{LP-BM5} < 0.001$, $p_{group} = 0.047$, $p_{LP-BM5 \times group} = 0.124$; and Fig. 1c, serum IgG2a, $p_{LP-BM5} < 0.001$, $p_{group} = 0.010$, $p_{LP-BM5 \times group} = 0.708$). For serum IgG2a, *post-hoc* analysis identified significant group differences between old gp120tg+ vs. both of the young gp120tg groups (Tukey test: $p < 0.05$ for both). For serum IgM, *post-hoc* analysis identified significant group differences between old gp120tg- vs. all other groups within LP-BM5 treatment (Tukey test: $p < 0.05$ for all). For splenic viral load, all LP-BM5 treated groups had detectable BM5Def expression while BM5Def was non-detectable in non-LP-BM5 treated groups (One-way ANOVA: Fig. 2a, spleen BM5Def, $p_{group} = 0.006$). Old gp120tg- group had lower splenic viral load than both the young gp120tg groups (Dunn’s test: $p < 0.05$ for both). All together, we were confident that immunodeficiency could be established in both gp120tg+ and gp120tg- mice following LP-BM5 treatment.

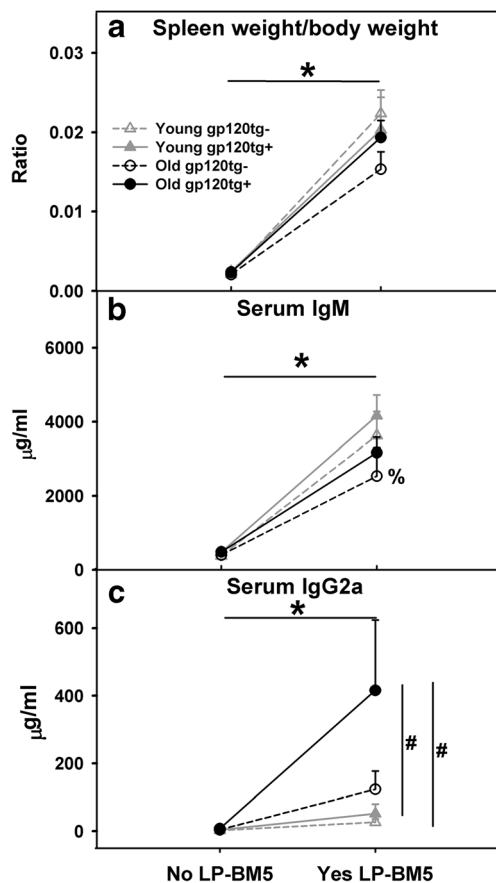


Fig. 1 Development of immunodeficiency in gp120tg mice treated with LP-BM5. Young (8–10 week old) and old (4–5 months old) gp120tg+ and gp120tg- mice were euthanized at 12 weeks post-LP-BM5 treatment (5×10^4 pfu, i.p.). Spleen weight/body weight ratio (a), serum IgM (b), and serum IgG2a (c) are shown in interaction plots. Data are presented as mean \pm SEM; $n = 7$ –16/group. Two-way ANOVA followed by Tukey post hoc test were performed. * indicates the main effect of LP-BM5 ($p < 0.05$). # $p < 0.05$ between the indicated groups regardless of LP-BM5 treatment. % $p < 0.05$ between the indicated group and all other groups under LP-BM5 treatment condition only

BM5def and gp120 Expression in the CNS of gp120tg Mice

HIV enters the CNS within 2 weeks of infection in patients and can often be detected despite suppressed serum viral load under antiviral treatment (Spudich et al. 2019; Williams et al. 2014), therefore it is critical to exam whether LP-BM5 entered the CNS of gp120tg mice in addition to causing systemic immunodeficiency. While without LP-BM5 treatment, BM5Def was not detectable, BM5Def RNA expression was detected in all three brain regions examined (hippocampus, frontal lobe and striatum) following LP-BM5 treatment regardless of gp120 expression or age (One-way on rank (log transformed data for all): Fig. 2b, hippocampus BM5Def, $p_{group} = 0.249$; Fig. 2c, frontal lobe BM5Def, $p_{group} = 0.046$; Fig. 2d, striatum BM5Def, $p_{group} = 0.796$). This indicates that LP-BM5 was able to penetrate the CNS of gp120tg mice

while causing systemic immunodeficiency. Thus, we were able to examine gp120-induced neuroimmune responses under systemic immunodeficient conditions in the presence of a murine retrovirus in the CNS.

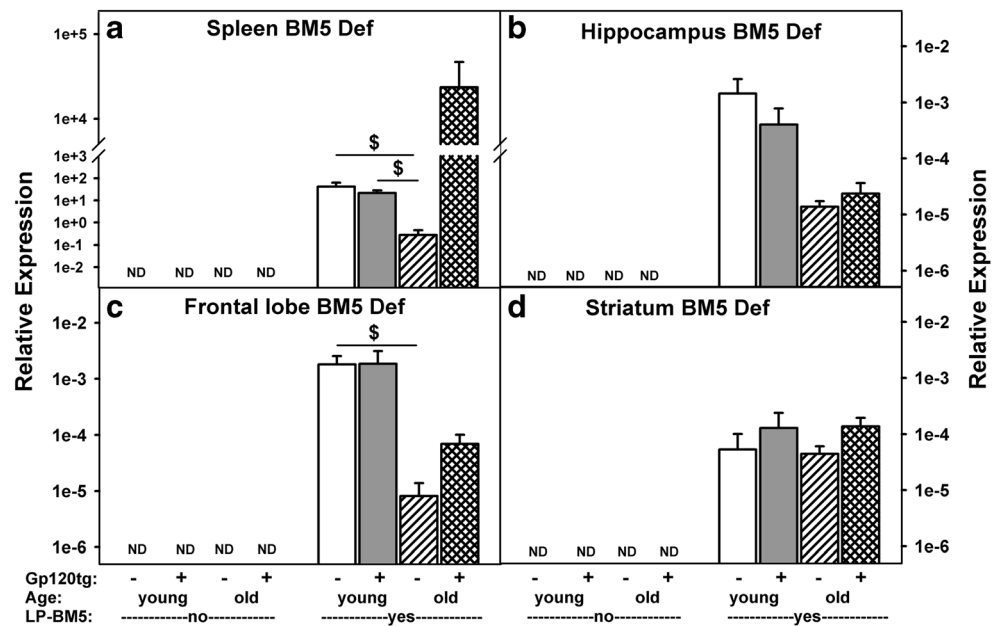
Expression of gp120 was also evaluated to detect any potential modifications by LP-BM5 treatment. Overall, the level of gp120 RNA matched the group identity (gp120tg+ vs. gp120tg-) and older mice showed higher levels of gp120 RNA than that of young mice, particularly in hippocampus and striatum (Two-way ANOVA: Fig. 3a, hippocampus gp120, $p_{LP-BM5} = 0.477$, $p_{group} < 0.001$, $p_{LP-BM5 \times group} = 0.250$; Fig. 3b, frontal lobe gp120, $p_{LP-BM5} = 0.241$, $p_{group} < 0.001$, $p_{LP-BM5 \times group} = 0.616$; Fig. 3c, striatum gp120, $p_{LP-BM5} = 0.829$, $p_{group} < 0.001$, $p_{LP-BM5 \times group} = 0.786$. For all three brain regions Tukey test: $p < 0.05$ between either of the young or old gp120tg+ groups vs. both gp120tg- mice).

RNA Expression of pro-Inflammatory Mediators in the CNS of gp120tg Mice in Immunodeficient vs. Immunocompetent States

Several pro-inflammatory mediators such as CCL2, CCL3, CCL4, CCL5, CXCL10, iNOS, IL-1 β , IL-6, TNF α , and IL-12 have been reported to contribute to the development of HAND in humans, as well as in many animal models for HAND (Asensio et al. 2001; Brabers and Nottet 2006; Cary et al. 2013; Kolb et al. 1999; Sivro et al. 2014; Watanabe et al. 2010). Therefore, we assessed the RNA levels of many of these factors in our experimental system using qRT-PCR.

Among the β chemokines, CCL3, CCL4, and CCL5 are ligands to the CCR5 receptor (host cell HIV-1 co-receptor) and are described together. Within the hippocampus, main effects of infection and group were detected for CCL5 (Two-way ANOVA: Fig. 4a, hippocampus CCL5, $p_{LP-BM5} = 0.015$, $p_{group} = 0.004$, $p_{LP-BM5 \times group} = 0.171$). CCL5 expression was significantly induced with LP-BM5 treatment. Group differences were observed between young gp120tg+ vs. both old gp120tg groups (Tukey test: $p < 0.05$ for both) with the highest levels of CCL5 expression found in LP-BM5-treated, young gp120tg+ mice (Tukey test: under LP-BM5 treated condition, $p < 0.05$ between young gp120tg+ vs. both old gp120tg groups). In the striatum, the main inductive effect was observed with LP-BM5 treatment without any group differences (Two-way ANOVA: Fig. 4c, striatum CCL5, $p_{LP-BM5} = 0.008$, $p_{group} = 0.241$, $p_{LP-BM5 \times group} = 0.771$). In the frontal lobe, only significant group differences (no LP-BM5 main effect) between young gp120tg+ and old gp120tg- mice were detected (Two-way ANOVA: Fig. 4b, frontal lobe CCL5, $p_{LP-BM5} = 0.246$, $p_{group} = 0.011$, $p_{LP-BM5 \times group} = 0.2401$, and Tukey test: $p < 0.05$), with CCL5 expression higher in young gp120tg+ mice prior to LP-BM5 treatment (Tukey test: without LP-BM5 treatment, $p < 0.05$ between young gp120tg+ vs. both young and old gp120tg- groups).

Fig. 2 BM5Def expression in the spleen and CNS of gp120tg mice. Young (8–10 week old) and old (4–5 months old) gp120tg + and gp120tg- mice were euthanized at 12 weeks post-LP-BM5 treatment (5×10^4 pfu, i.p.). BM5 Def viral loads for spleen (a), hippocampus (b), frontal lobe (c), and striatum (d) are shown here. Data are presented as mean \pm SEM; $n = 7$ –16/group. One-way ANOVA on rank followed by Dunn's *post hoc* test were performed with groups that were treated with LP-BM5. \$ $p < 0.05$ between the indicated groups. ND = not detectable



With regard to CCL4, although significant main inductive effects from LP-BM5 were detected in the hippocampus and striatum (striatum had higher levels of CCL4 than the other two brain regions), no significant group main effect was identified (Two-way ANOVA: Fig. 4d, hippocampus CCL4, $p_{LP-BM5} = 0.005$, $p_{group} = 0.101$, $p_{LP-BM5 \times group} = 0.832$; Fig. 4f, striatum CCL4, $p_{LP-BM5} = 0.050$, $p_{group} = 0.597$, $p_{LP-BM5 \times group} = 0.555$). In the frontal lobe, only a significant group difference (no LP-BM5 main effect) between old gp120tg+ and young gp120tg- mice was detected (Two-way ANOVA: Fig. 4e, frontal lobe CCL4, $p_{LP-BM5} = 0.938$, $p_{group} = 0.002$, $p_{LP-BM5 \times group} = 0.079$, followed by Tukey test: $p < 0.05$). Similar to CCL5, there appeared to be a trend towards a gp120-associated increase of frontal lobe CCL4 in young mice (Tukey test: without LP-BM5 treatment, $p < 0.05$ between young gp120tg+ vs. both young and old gp120tg- groups), which was reduced following LP-BM5 treatment. No significant main effect from LP-BM5 was observed with CCL3 expression in any of the three brain regions examined (Two-way ANOVA: Fig. 4g, hippocampus CCL3, $p_{LP-BM5} = 0.361$, $p_{group} = 0.123$, $p_{LP-BM5 \times group} = 0.200$; Fig. 4i, striatum CCL4, $p_{LP-BM5} = 0.300$, $p_{group} = 0.453$, $p_{LP-BM5 \times group} = 0.553$; Fig. 4h, frontal lobe CCL3, $p_{LP-BM5} = 0.592$, $p_{group} = 0.025$, $p_{LP-BM5 \times group} = 0.911$). The significant group main effect in the frontal lobe was seen between the young gp120tg+ and old gp120tg- mice where young gp120tg+ mice appeared to have the highest levels of CCL3 expression among all groups regardless of LP-BM5 treatment (Tukey test: $p < 0.05$).

For both CCL2 and CXCL10, we observed significant gp120-related increases in all three brain regions which were not significantly affected by LP-BM5-induced systemic immunodeficiency or the presence of LP-BM5 within the CNS.

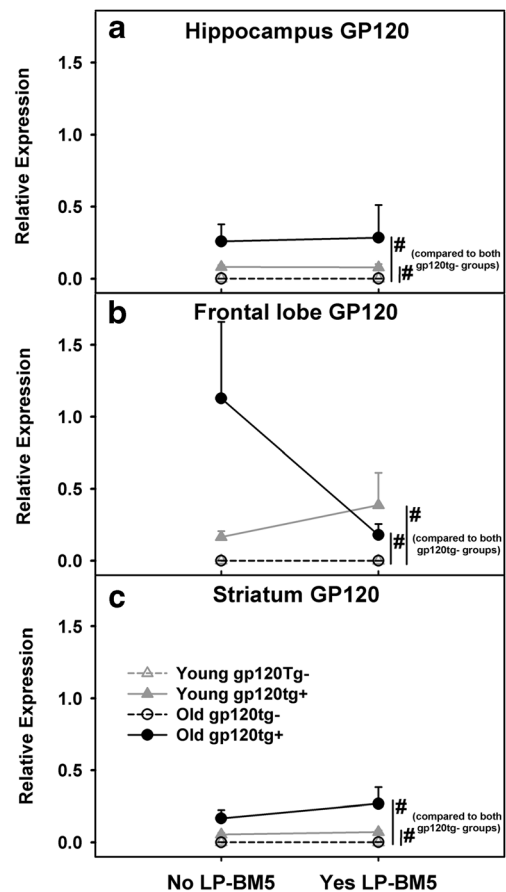


Fig. 3 RNA expression of gp120 in the CNS of immunocompetent vs. immunocompromised gp120tg mice. Young (8–10 week old) and old (4–5 months old) gp120tg + and gp120tg- mice were euthanized at 12 weeks post-LP-BM5 treatment (5×10^4 pfu, i.p.). RNA expression of gp120 in the hippocampus (a), frontal lobe (b), and striatum (c) are shown in interaction plots. Data are presented as mean \pm SEM; $n = 7$ –16/group. Two-way ANOVA followed by Tukey *post hoc* test were performed. # $p < 0.05$ between the indicated groups regardless of LP-BM5 treatment

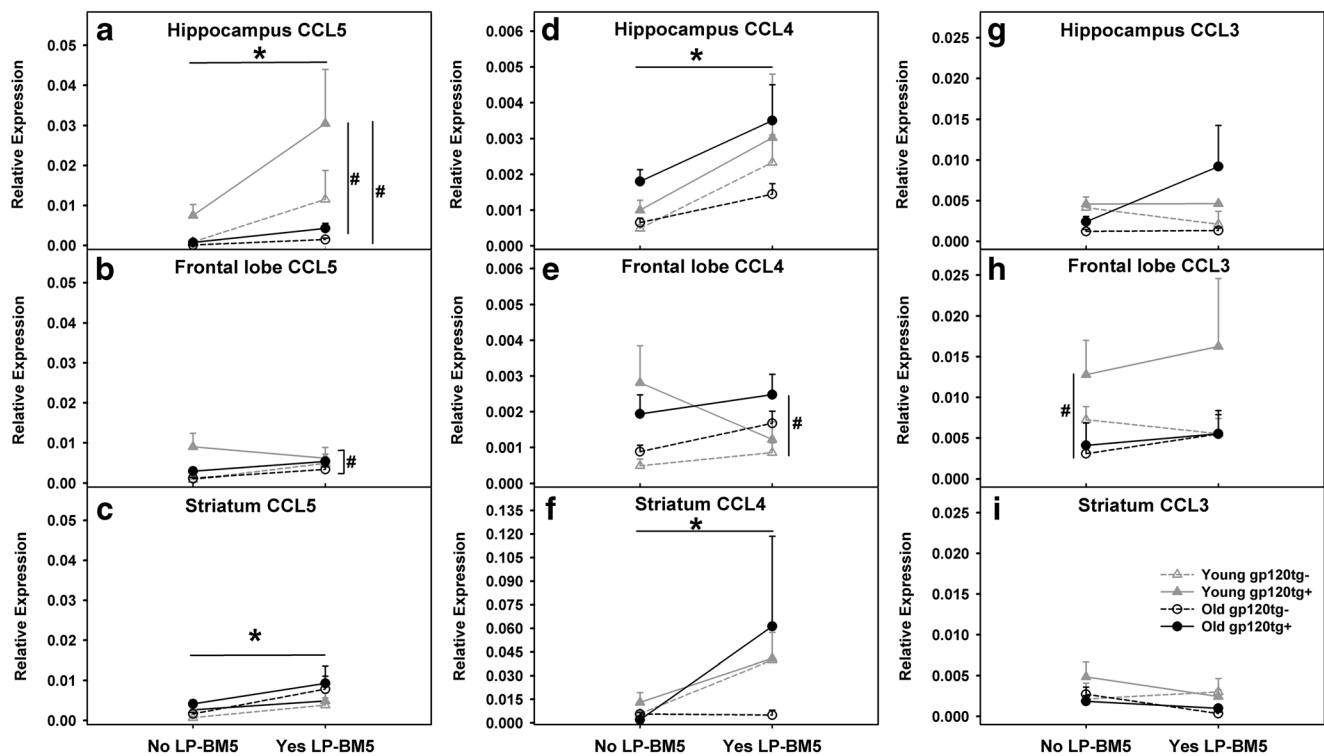


Fig. 4 RNA expression of CCL5, CCL4, and CCL3 in the CNS of immunocompetent vs. immunocompromised gp120tg mice. Young (8–10 week old) and old (4–5 months old) gp120tg+ and gp120tg- mice were euthanized at 12 weeks post-LP-BM5 treatment (5×10^4 pfu, i.p.). RNA expression of CCL5 (a–c), CCL4 (d–f), and CCL3 (g–i) in the

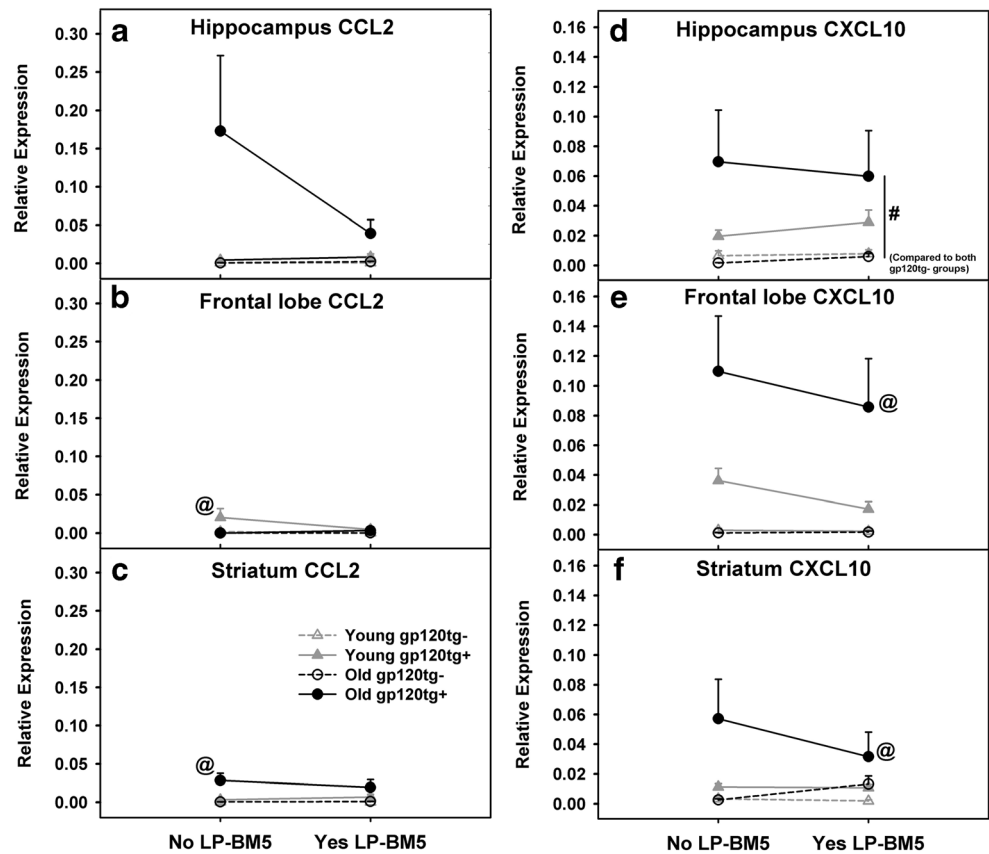
hippocampus (a, d and g), frontal lobe (b, e and h) and striatum (c, f, and i) are shown in interaction plots. Data are presented as mean \pm SEM; $n = 7–16$ /group. Two-way ANOVA followed by Tukey *post hoc* test were performed. * indicates the main effect of LP-BM5 ($p < 0.05$). # $p < 0.05$ between the indicated groups regardless of LP-BM5 treatment

Specifically, old gp120tg+ mice had higher levels of CCL2 expression in the striatum and higher levels of CXCL10 expression in all three brain regions compared to all other groups with a decreasing trend following LP-BM5 treatment (Two-way ANOVA: Fig. 5c, striatum CCL2, $p_{LP-BM5} = 0.712$, $p_{group} < 0.001$, $p_{LP-BM5 \times group} = 0.639$; Fig. 5d, hippocampus CXCL10, $p_{LP-BM5} = 0.912$, $p_{group} = 0.002$, $p_{LP-BM5 \times group} = 0.951$; Fig. 5e, frontal lobe CXCL10, $p_{LP-BM5} = 0.362$, $p_{group} < 0.001$, $p_{LP-BM5 \times group} = 0.836$; Fig. 5f, striatum CXCL10, $p_{LP-BM5} = 0.614$, $p_{group} = 0.003$, $p_{LP-BM5 \times group} = 0.455$; for Figs. 5c, e and f, Tukey test: $p < 0.05$ between old gp120tg+ mice and all other groups; for Fig. 5d, Tukey test: $p < 0.05$ between old gp120tg+ mice and both of the gp120tg- groups). Hippocampal CCL2 expression levels were also elevated in the old gp120tg+ group compared to all other groups (also with a decreasing trend with LP-BM5 treatment), however with weaker statistical results in *post-hoc* analysis (Two-way ANOVA: Fig. 5a, hippocampus CCL2, $p_{LP-BM5} = 0.264$, $p_{group} = 0.026$, $p_{LP-BM5 \times group} = 0.244$, and Tukey test: p values ranged between 0.05 to 0.01 when the old gp120tg+ group was compared to all other groups, yet, under non-LP-BM5 treated condition, $p < 0.05$ between old gp120tg+ mice and all other groups). In the frontal lobe, the young gp120tg+ mice had significantly elevated CCL2 expression levels compared to all other groups (Two-way

ANOVA: Fig. 5b, frontal lobe CCL2, $p_{LP-BM5} = 0.175$, $p_{group} = 0.004$, $p_{LP-BM5 \times group} = 0.059$, and Tukey test: $p < 0.05$ between young gp120tg+ mice and all other groups), which also showed a decreasing trend with LP-BM5 treatment.

Other pro-inflammatory factors examined include iNOS, TNF α , and IL-12p40. Although no significant changes in iNOS was detected in the hippocampus (Two-way ANOVA: Fig. 6a, hippocampus iNOS, $p_{LP-BM5} = 0.634$, $p_{group} = 0.282$, $p_{LP-BM5 \times group} = 0.805$), LP-BM5 had significant inductive main effects in TNF α and IL-12p40 expression (Two-way ANOVA: Fig. 6d, hippocampus TNF α , $p_{LP-BM5} = 0.019$, $p_{group} = 0.074$, $p_{LP-BM5 \times group} = 0.113$; Fig. 6g, hippocampus IL-12p40, $p_{LP-BM5} = 0.002$, $p_{group} = 0.060$, $p_{LP-BM5 \times group} = 0.033$), with old gp120tg+ mice showing the greatest increase following LP-BM5 treatment (Tukey test: for TNF α , under LP-BM5 treatment, $p < 0.05$ between old gp120tg+ vs. both young gp120tg groups; for IL-12p40, under LP-BM5 treatment, $p < 0.05$ between old gp120tg+ vs. both old and young gp120tg- groups). Age-dependent changes induced by LP-BM5 were also observed in the striatum, where a significant interaction between LP-BM5 and group was observed. Striatal iNOS expression in old gp120tg+ mice was significantly elevated following LP-BM5 treatment compared to expression levels in both of the young gp120tg groups (Two-way ANOVA: Fig. 6c, striatum iNOS, p_{LP-

Fig. 5 RNA expression of CCL2 and CXCL10 in the CNS of immunocompetent vs. immunocompromised gp120tg mice. Young (8–10 week old) and old (4–5 months old) gp120tg+ and gp120tg- mice were euthanized at 12 weeks post-LP-BM5 treatment (5×10^4 pfu, i.p.). RNA expression of CCL2 (a–c) and CXCL10 (d–f) in the hippocampus (a and d), frontal lobe (b and e), and striatum (c and f) are shown in interaction plots. Data are presented as mean \pm SEM; $n = 7$ –16/group. Two-way ANOVA followed by Tukey *post hoc* test were performed. # $p < 0.05$ between the indicated groups regardless of LP-BM5 treatment. @ $p < 0.05$ between the indicated group and all other groups regardless of LP-BM5 treatment



$BM5 = 0.366$, $p_{group} = 0.022$, $p_{LP-BM5 \times group} = 0.049$, and Tukey test: under LP-BM5 treatment, $p < 0.05$ between old gp120tg+ LP-BM5 vs. both young gp120tg LP-BM5 groups). It should be noted that iNOS expression levels were much higher in striatum than that in the hippocampus and frontal lobe. While no inductive effects of LP-BM5 were statistically significant in striatal TNF α expression (Two-way ANOVA: Fig. 6f, striatum TNF α , $p_{LP-BM5} = 0.630$, $p_{group} = 0.214$, $p_{LP-BM5 \times group} = 0.130$), a main effect of LP-BM5 was detected in IL-12p40 expression in the striatum (Two-way ANOVA: Fig. 6i, striatum IL-12p40, $p_{LP-BM5} = 0.026$, $p_{group} = 0.073$, $p_{LP-BM5 \times group} = 0.109$) and young gp120tg+ mice appeared to have the greatest increase in IL-12p40 following LP-BM5 treatment (Tukey test; under LP-BM5 treatment, $p < 0.05$ between young gp120tg+ mice vs. both of the old gp120tg groups). For the frontal lobe, group differences were more notable than the effects from LP-BM5. Old gp120tg+ mice had higher expression levels of iNOS (Two-way ANOVA: Fig. 6b, frontal lobe iNOS, $p_{LP-BM5} = 0.312$, $p_{group} < 0.001$, $p_{LP-BM5 \times group} = 0.355$, and Tukey test: $p < 0.05$ between the old gp120tg+ mice and both of the young gp120tg groups) while young gp120tg+ mice had higher expression levels in both TNF α and IL-12p40 (Two-way ANOVA: Fig. 6e, frontal lobe TNF α , $p_{LP-BM5} = 0.268$, $p_{group} = 0.028$, $p_{LP-BM5 \times group} = 0.643$, and Tukey test: $p < 0.05$ between young gp120tg+ and old

gp120tg- group; Fig. 6h, frontal lobe IL-12p40, $p_{LP-BM5} = 0.046$, $p_{group} = 0.005$, $p_{LP-BM5 \times group} = 0.151$, and Tukey test: $p < 0.05$ between young gp120tg+ and both old gp120tg groups). Further, the significant main effect from LP-BM5 indicated a decrease in IL-12p40 expression in the frontal lobe following LP-BM5 treatment, particularly for the young gp120tg+ group (Fig. 6h, Tukey test: without LP-BM5 treatment, $p < 0.05$ between young gp120tg+ mice vs. both of the old gp120tg groups).

RNA Expression of Type I and Type II IFNs in the CNS of gp120tg Mice in Immunodeficiency vs. Immunocompetent States

IFN α and IFN β are major mediators of the type I IFN response, an antiviral response within innate immunity. IFN α and IFN β revealed similar expression patterns in our model system. Young gp120tg- mice had the highest expression levels of type I IFN, which generally decreased with gp120 expression, age, and/or LP-BM5 treatment, however this decrease was dependent upon the specific type I IFN and brain region examined (Two-way ANOVA: Fig. 7a, hippocampus IFN α , $p_{LP-BM5} = 0.272$, $p_{group} = 0.001$, $p_{LP-BM5 \times group} = 0.157$, and Tukey test: $p < 0.05$ between young gp120tg- mice vs. all other groups; Fig. 7b, frontal lobe IFN α , $p_{LP-BM5} = 0.384$, $p_{group} = 0.006$, $p_{LP-BM5 \times group} = 0.940$, and Tukey test: $p < 0.05$

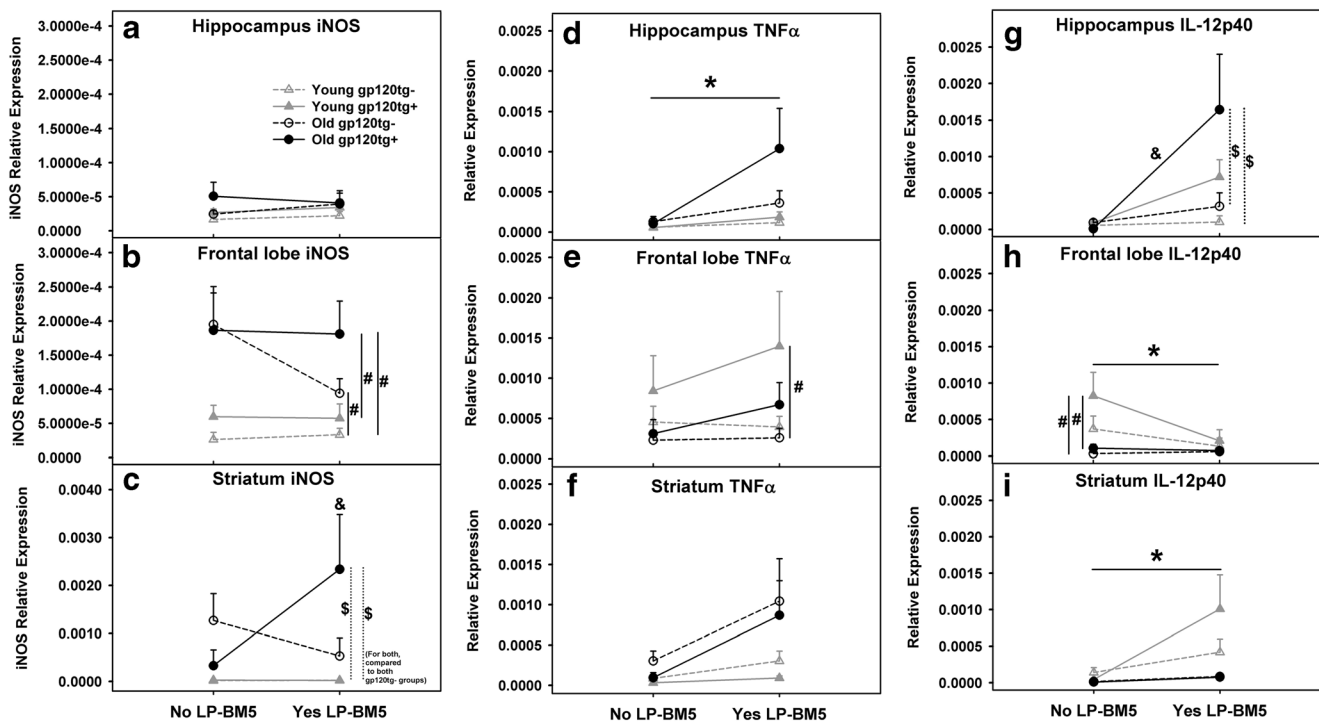


Fig. 6 RNA expression of iNOS, TNF α , and IL-12p40 in the CNS of immunocompetent vs. immunocompromised gp120tg mice. Young (8–10 week old) and old (4–5 months old) gp120tg+ and gp120tg- mice were euthanized at 12 weeks post-LP-BM5 treatment (5×10^4 pfu, i.p.). RNA expression of iNOS (a–c), TNF α (d–f), and IL-12p40 (g–i) in the hippocampus (a, d and g), frontal lobe (b, e, and h), and striatum (c, f, and i) are shown in interactive plots. Data are presented as mean \pm SEM; $n = 7$ –16/

group. Two-way ANOVA followed by Tukey *post hoc* test were performed. * indicates the main effect of LP-BM5 ($p < 0.05$). # $p < 0.05$ between the indicated groups regardless of LP-BM5 treatment. \$ $p < 0.05$ between indicated groups under LP-BM5 treatment condition only. & $p < 0.05$ between LP-BM5 treated vs. non treated mice of the indicated group

between young gp120tg- mice vs. both old gp120tg groups; Fig. 7c, striatum IFN α , $p_{LP-BM5} = 0.386$, $p_{group} = 0.865$, $p_{LP-BM5 \times group} = 0.063$; Fig. 7d, hippocampus IFN β , $p_{LP-BM5} = 0.723$, $p_{group} = 0.002$, $p_{LP-BM5 \times group} = 0.342$, and Tukey test: $p < 0.05$ between young gp120tg- mice vs. all other groups; Fig. 7e, frontal lobe IFN β , $p_{LP-BM5} = 0.213$, $p_{group} = 0.074$, $p_{LP-BM5 \times group} = 0.775$; Fig. 7f, striatum IFN β , $p_{LP-BM5} = 0.030$, $p_{group} = 0.294$, $p_{LP-BM5 \times group} = 0.083$, and Tukey test: within non-LP-BM5 treated groups, $p < 0.05$ between young gp120tg- mice vs. both old gp120tg groups). With regard to IFN γ , group main effects were detected in the hippocampus and frontal lobe. In the hippocampus, significant differences were detected between the old gp120tg+ vs. the old gp120tg- and the young gp120tg+ group, with the old gp120tg+ group showing increased IFN γ expression following LP-BM5 treatment compared to the other groups (Two-way ANOVA: Fig. 7g, hippocampus IFN γ , $p_{LP-BM5} = 0.270$, $p_{group} = 0.004$, $p_{LP-BM5 \times group} = 0.507$, and Tukey test: $p < 0.05$ between the old gp120tg+ vs. the old gp120tg- and the young gp120tg+ groups, while under LP-BM5 treatment only, $p < 0.05$ between old gp120tg+ mice vs. all other groups). In the frontal lobe, LP-BM5 induced IFN γ expression regardless of genotype and age (Two-way ANOVA: Fig. 7h, frontal lobe IFN γ , $p_{LP-BM5} = 0.005$,

$p_{group} = 0.862$, $p_{LP-BM5 \times group} = 0.904$). Although a statistically significant interaction between LP-BM5 and group was found in IFN γ expression within the striatum, no significant group differences were detected in the *post-hoc* analyses (Two-way ANOVA: Fig. 7i, striatum IFN γ , $p_{LP-BM5} = 0.309$, $p_{group} = 0.346$, $p_{LP-BM5 \times group} = 0.031$).

RNA Expression of CD11b and GFAP in the CNS of gp120tg Mice in Immunodeficiency vs. Immunocompetent States

To further delineate the brain region-specific responses in inflammatory cytokines/chemokines observed above, we examined the expression of CD11b (representing microglia) and GFAP (representing astrocytes) (Fig. 8). Although no meaningful changes were identified in CD11b RNA expression in any of the brain regions examined (Two-way ANOVA: Fig. 8a, hippocampus CD11b, $p_{LP-BM5} = 0.217$, $p_{group} = 0.650$, $p_{LP-BM5 \times group} = 0.555$; Fig. 8b, frontal lobe CD11b, $p_{LP-BM5} = 0.656$, $p_{group} = 0.315$, $p_{LP-BM5 \times group} = 0.715$; Fig. 8c, striatum CD11b, $p_{LP-BM5} = 0.713$, $p_{group} = 0.033$, $p_{LP-BM5 \times group} = 0.951$, and Tukey test: $p < 0.05$ between young gp120tg- vs. old gp120tg- mice), RNA expression of GFAP was much higher in the gp120tg+ mice in hippocampus compared to

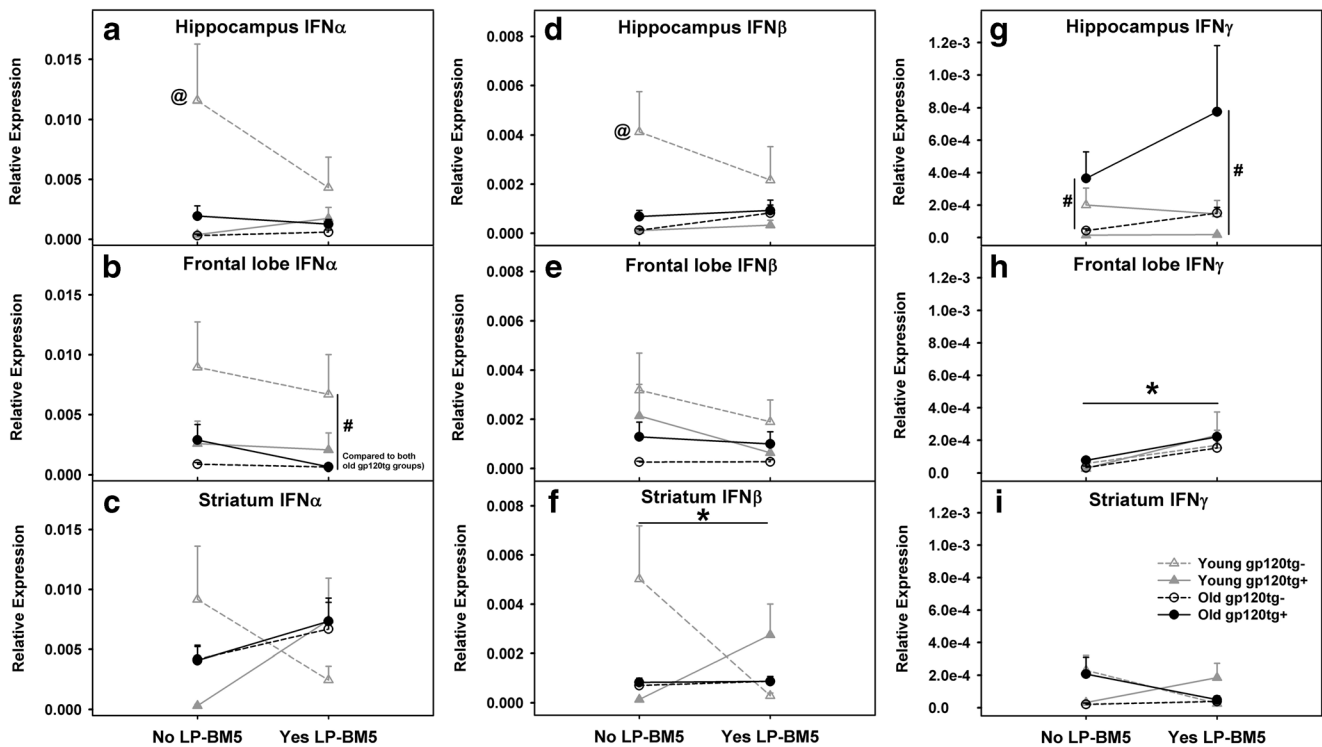


Fig. 7 RNA expression of IFN α , IFN β , and IFN γ in the CNS of immunocompetent vs. immunocompromised gp120tg mice. Young (8–10 week old) and old (4–5 months old) gp120tg+ and gp120tg- mice were euthanized at 12 weeks post-LP-BM5 treatment (5×10^4 pfu, i.p.). RNA expression of IFN α (a–c), IFN β (d–f), and IFN γ (g–i) in the hippocampus (a, d and g), frontal lobe (b, e, and h), and striatum (c, f, and i) are

shown in interaction plots. Data are presented as mean \pm SEM; $n = 7–16$ /group. Two-way ANOVA followed by Tukey *post hoc* test were performed. * indicates the main effect of LP-BM5 ($p < 0.05$). # $p < 0.05$ between the indicated groups regardless of LP-BM5 treatment. @ $p < 0.05$ between the indicated group and all other groups regardless of LP-BM5 treatment

the other two brain regions or groups, which may suggest greater astrocytic activation in hippocampus (Two way ANOVA: Fig. 8d, hippocampus GFAP, $p_{LP-BM5} = 0.790$, $p_{group} = 0.001$, $p_{LP-BM5 \times group} = 0.675$, and Tukey test: $p < 0.05$ between old gp120tg- vs. both young and old gp120tg+ groups; Fig. 8e, frontal lobe GFAP, $p_{LP-BM5} = 0.475$, $p_{group} < 0.001$, $p_{LP-BM5 \times group} = 0.248$, and Tukey test: $p < 0.05$ between each of the young or old gp120tg+ groups vs. each of the old and young gp120tg- mice, same group differences were also seen in LP-BM5 treated mice; Fig. 8f, striatum GFAP, $p_{LP-BM5} = 0.327$, $p_{group} = 0.022$, $p_{LP-BM5 \times group} = 0.704$, and Tukey test: $p < 0.05$ between young gp120tg- vs. old gp120tg+ mice).

Expression of Synaptophysin and MAP2 in the CNS of gp120tg Mice in Immunodeficiency vs. Immunocompetent States

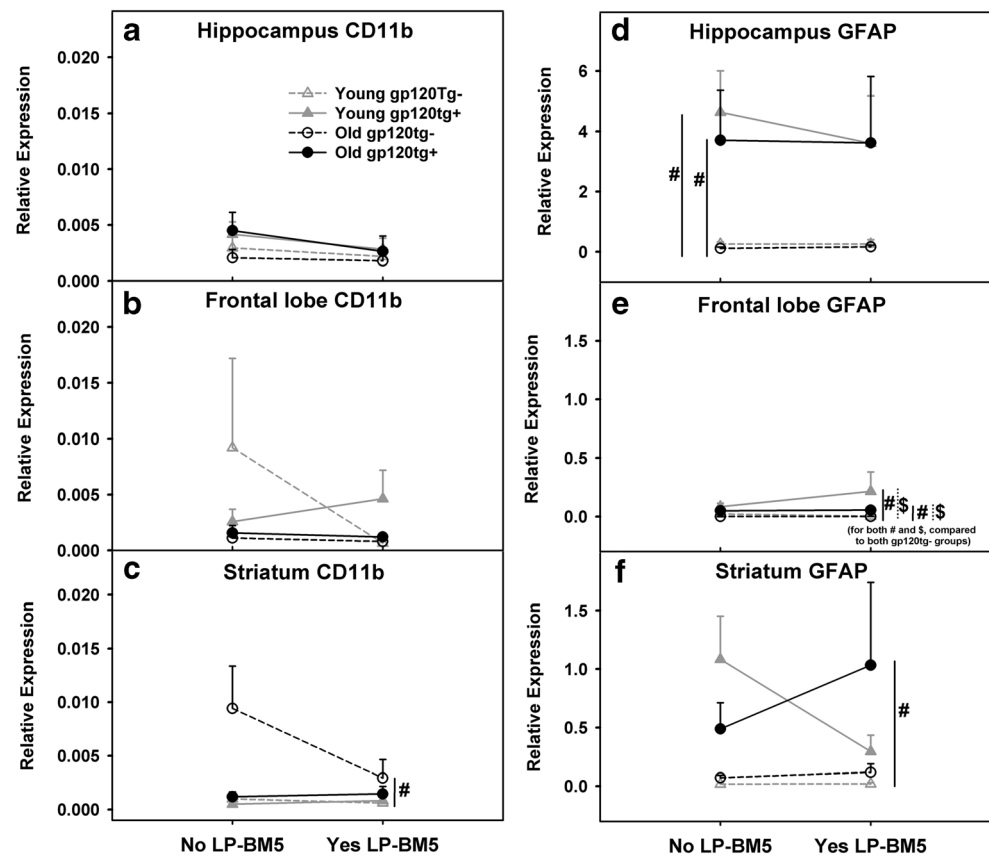
It has been shown that hippocampal levels of synaptophysin and MAP-2 are significantly lower in gp120tg+ compared to gp120tg- mice (Thaney et al. 2017). We examined the protein levels of synaptophysin and MAP2 in the hippocampus via ELISA (Fig. 9). For synaptophysin, although no significant effects from LP-BM5 treatment was observed, we did observe

a significant overall reduction induced with the presence of gp120 and an age-related increase of synaptophysin, where a greater level of synaptophysin was detected in older mice (Three-way ANOVA: Fig. 9a, hippocampus synaptophysin, $p_{LP-BM5} = 0.629$, $p_{gp120} = 0.010$, $p_{age} < 0.001$; Tukey test: $p < 0.05$ between gp120tg+ vs. gp120tg- mice within both young and old mice, and $p < 0.05$ between young vs. old within gp120tg- mice). For MAP2, we also detected a significant age-related effect, with decreased MAP2 expression in older mice (Three-way ANOVA: Fig. 9b, $p_{gp120} = 0.901$, $p_{age} < 0.001$, and $p_{LP-BM5} = 0.191$). Similar age-related changes in hippocampal synaptophysin and MAP2 expression have been reported previously (Benice et al. 2006; Chauhan and Siegel 1997; Di Stefano et al. 2001; Eastwood et al. 2006; Yu et al. 2011). In addition, we measured the expression of synaptophysin and MAP2 at the RNA level. No significant group differences were detected (data not shown).

Assessment of Cognitive Function Using the Spontaneous Alternation T-Maze Behavioral Assay

The spontaneous alternation T-maze assay was used (during the 12th week post-LP-BM5) to assess potential learning/memory deficits, specifically related to hippocampal function

Fig. 8 RNA expression of CD11b and GFAP in the CNS of immunocompetent vs. immunocompromised gp120tg mice. Young (8–10 week old) and old (4–5 months old) gp120tg+ and gp120tg- mice were euthanized at 12 weeks post-LP-BM5 treatment (5×10^4 pfu, i.p.). RNA expression of CD11b (a–c) and GFAP (d–f) in the hippocampus (a and d), frontal lobe (b and e), and striatum (c and f) are shown in interaction plots. Data are presented as mean \pm SEM; $n = 7$ – 16 /group. Two-way ANOVA followed by Tukey *post hoc* test were performed. # $p < 0.05$ between the indicated groups regardless of LP-BM5 treatment. \$ $p < 0.05$ between indicated groups under LP-BM5 treatment condition only



(Deacon and Rawlins 2006) in gp120tg mice with or without LP-BM5. For each mouse, we measured both percent correct (for assessing learning/memory function) and the time to choice (for exclusion of potential motor function deficits or lack of motivation) for both 0- and 2 min retention times (increased retention time provides increased learning/memory burden) (Deacon and Rawlins 2006; Lee and Kesner 2003). First, when outcome measures were compared based on the time intervals, 2 min interval significantly decreased the percent correct (Wilcoxon Signed Rank Test: Fig. 10a and b, percent correct, $p = 0.005$) but did not affect the time to choice (Wilcoxon Signed Rank Test: Fig. 10c and d, time to choice, $p = 0.5$). Regarding the performance, a main effect of LP-BM5 treatment was detected, i.e. LP-BM5 decreased the percent of correct choices made following a 0 min retention interval (Two-way-ANOVA: Fig. 10a, 0 min percent correct, $p_{LP-BM5} = 0.008$, $p_{group} = 0.432$, $p_{LP-BM5 \times group} = 0.088$). When the 2 min interval was used, no LP-BM5 effect was observed, while group differences between young gp120tg+ mice vs. both of the old gp120tg groups were detected indicating potential age-related impairment (Two-way ANOVA: Fig. 10b, 2 min percent correct, $p_{LP-BM5} = 0.236$, $p_{group} < 0.001$, $p_{LP-BM5 \times group} = 0.674$, and Tukey test: $p < 0.05$ between young gp120tg+ mice vs. both of the old gp120tg groups). When the time to choice was analyzed, group main effects were detected in both 0- and

2 min retention times. However the *post-hoc* test only identified a difference between the young gp120tg- and the old gp120tg+ mice following a 0-min retention time (Two-way ANOVA: Fig. 10c, 0 min time to choice, $p_{LP-BM5} = 0.315$, $p_{group} = 0.009$, $p_{LP-BM5 \times group} = 0.302$, and Tukey test: $p < 0.05$ between young gp120tg- vs. old gp120tg+ mice; Fig. 10d, 2 min time to choice, $p_{LP-BM5} = 0.946$, $p_{group} = 0.023$, $p_{LP-BM5 \times group} = 0.574$, and Tukey test: $p > 0.05$ for all).

Discussion

In this study we explored gp120-induced neuroinflammation in a state of immunodeficiency induced by a murine retrovirus (LP-BM5). Our goal was to better understand neuroinflammation of different brain regions, and how systemic immunodeficiency with CNS viral presence affects the behavior of the gp120 viral protein in the CNS. According to the CDC, only 30% of HIV patients in the US have viral loads that are controlled by antiretroviral therapy (Bradley et al. 2014), suggesting the relevance of studying viral responses under immunodeficient conditions. Thus, the presence of gp120 in the CNS of LP-BM5-treated mice could be used to understand gp120-induced responses in HIV-infected individuals with uncontrolled viral loads. Further, despite the wide use of antiviral treatment, the prevalence of HAND remains high. HIV can

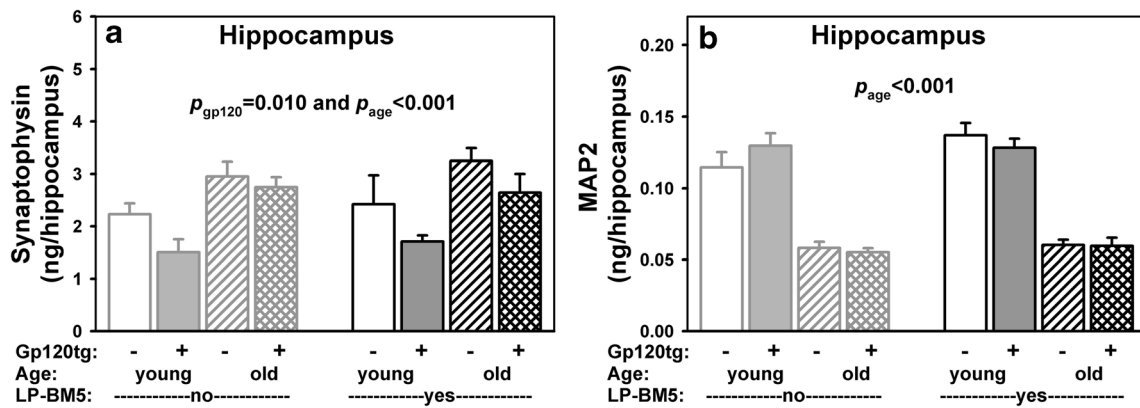


Fig. 9 Synaptophysin and MAP2 expression in the hippocampus of immunocompetent vs. immunocompromised gp120tg mice. Young (8–10 week old) and old (4–5 months old) gp120tg+ and gp120tg- mice were euthanized at 12 weeks post-LP-BM5 treatment (5×10^4 pfu, i.p.).

Hippocampal expression of synaptophysin (a) and MAP2 (b) at protein levels are shown here. Data are presented as mean \pm SEM; $n = 6$ – 10 /group. Results of three-way ANOVA are shown within the graph

persist in the brain even with satisfactory control of the viral load in the periphery (McArthur et al. 2010; Saylor et al. 2016). A recent study showed that nearly 50% of HIV-infected individuals who have suppressed plasma HIV RNA and adequate CD4 levels still have detectable HIV infected cells in their CSF (Spudich et al. 2019). The co-existence of gp120 and LP-BM5 viral RNA in the CNS could be helpful in revealing gp120-induced responses that are unique to the presence of retrovirus.

In the present study, gp120 neuroinflammation showed strong regional specificity. These differences were first observed when comparing the basal levels (without LP-BM5

treatment) of mRNA expression for each factor, which were often affected by age and gp120tg expression differently depending on the brain region studied – e.g., CCL4 and iNOS were significantly higher in the striatum than in other brain regions. LP-BM5 treatment-induced expression patterns of many pro-inflammatory factors varied significantly between regions. In the hippocampus, under LP-BM5 treatment, gp120 appeared to induce the expression of many pro-inflammatory factors including, CCL5 (in young mice), TNF α , IL-12p40 and IFN γ (mostly in old mice) with a reduction in CCL2 (in old mice). On the contrary, in the frontal lobe of gp120tg+ mice, LP-BM5 treatment appeared to be associated with

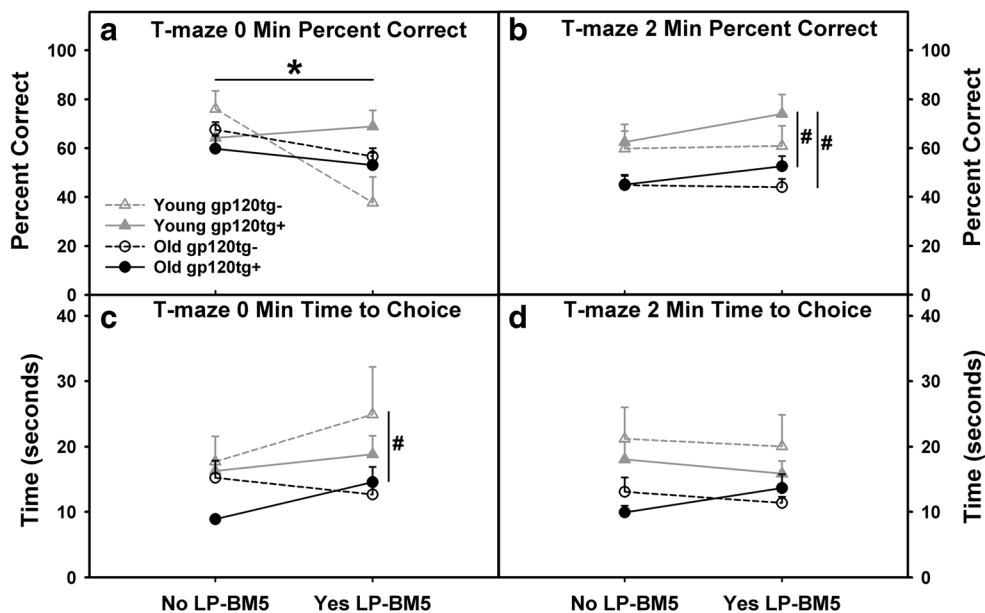


Fig. 10 Performance in the spontaneous alternative T-maze behavioral assay. Young (8–10 week old) and old (4–5 months old) gp120tg+ and gp120tg- mice were treated with LP-BM5 (5×10^4 pfu, i.p.) for 12 weeks. T-maze assay was performed during the 12th week of infection. Average percent correct choices made by each group during T-maze tests with 0 min (a) or 2 min (b) retention interval, as well as corresponding time

to choice for 0 min (c) and 2 min (d) are shown in interaction plots. Data are presented as mean \pm SEM; $n = 8$ – 20 /group. Two-way ANOVA followed by Tukey *post hoc* test were performed. * indicates the main effect of LP-BM5 ($p < 0.05$). # $p < 0.05$ between the indicated groups regardless of LP-BM5 treatment

reduced expression of many pro-inflammatory factors - particularly IL-12p40, and to some extent CCL5 and CCL2 - in young mice. Within the striatum, LP-BM5 in combination with gp120 further increased the expression of iNOS in old mice and IL-12p40 in young mice without substantially changing many other pro-inflammatory factors. Due to the limited amount of tissue available from each brain region of individual mice, we could not measure the changes of these cytokines/chemokines at the protein level. We realized that pattern of expression at the protein levels vs. RNA levels could be different (McLane et al. 2018). Nevertheless, our results suggest that under the condition of both retrovirus-induced systemic immunodeficiency and the presence of a retrovirus within the CNS, gp120 is more likely to mount a pro-inflammatory response in the hippocampus than in the striatum or frontal lobe, with the frontal lobe being the least likely region to display profound inflammatory changes. Therefore, one may predict that inflammation-related tissue damage is more likely to occur in the hippocampus under these conditions (which may occur more frequent than expected during the cART era (Bradley et al. 2014; Spudich et al. 2019)). This does not appear to be due to differential expression levels of gp120 in these brain regions (Fig. 3). However, differential glial responses, particularly the significantly higher hippocampal GFAP expression levels, indicate a greater level of hippocampal astrocytic activation which may contribute to the profound inflammatory responses within the hippocampus. Future studies could help delineate the cellular source of detected hippocampal pro-inflammatory cytokines/chemokines.

Interestingly, we also observed a significant gp120-associated reduction of hippocampal synaptophysin at the protein level. Synaptophysin has been used in previous studies as a marker for neuronal synaptic connections, with reduced levels seen in HIV-infected patients (Cantres-Rosario et al. 2019; Guha et al. 2018). Together, our results support the idea that the hippocampus is particularly susceptible to HIV, especially HIV gp120-induced neuroinflammation under the systemic immunodeficiency condition with the presence of a retrovirus in the CNS. This would in part explain the observed decline in executive function and learning and memory ability in patients with HAND (McArthur et al. 2010; Saylor et al. 2016). Increased inflammation in the hippocampus is consistent with other findings of ongoing inflammation that occurs in the hippocampus of patients treated with cART (Anthony et al. 2005). Other previous studies have also shown that peripheral blood mononuclear cells that entered the hippocampus of chronically infected HIV patients were more susceptible to mitochondrial oxidative damage and reduced hippocampal volume (Kallianpur et al. 2016). Unlike synaptophysin, we did not observe a gp120-dependent change in MAP2 at protein level, regardless of LP-BM5 treatment. Our results also showed that RNA expression of synaptophysin and MAP2 did not necessarily represent their expression at protein levels. MAP2 has high (>220KD) vs.

low (~70KD) molecular isoforms due to alternative splicing (Dehmelt and Halpain 2005; Kalcheva et al. 1995). If MAP2 remained insoluble within the lysis buffer (that did not contain sodium dodecyl sulfate) used, they would not be detected via ELISA. It's possible that gp120 or LP-BM5 effects were constrained to the insoluble MAP2 fraction. More detailed analysis of MAP2 using alternative methods would be beneficial in the future. Interestingly, LP-BM5 did not change protein levels of synaptophysin or MAP2, suggesting that the expressions of synaptophysin and MAP2 are not likely affected by the peripheral immune competency of the host.

Interestingly, gp120 alone did not cause a significant reduction in T maze performance and LP-BM5 treatment only led to impairment in T maze performance with 0 min retention regardless of gp120 expression. A broader spectrum of behavioral tests is warranted in order to reveal the behavioral consequences of the observed, seemingly more profound inflammatory responses in the hippocampus, as well as to identify changes in performance driven by other brain regions. Further, previous reports showed that gp120tg+ mice displayed memory/learning deficits between 9 and 12 months old (D'Hooge et al. 1999; Maung et al. 2014; Thaney et al. 2018). The mice in our study may be too young (at ~5 vs. 7–8 months old at the time of sample collection) to show any learning/memory deficits. In future studies, it would be interesting to examine mice that at 6–8 months old at the time of LP-BM5 treatment (i.e. sample collection at 9–11 months old) to determine whether gp120 would induce more significant learning/memory deficit under the immunodeficient conditions.

We also examined type I IFNs, which play a critical role in the antiviral response to HIV (Sivro et al. 2014). Consistent with a previous report that gp120tg+ mice lose type I IFN expression with age - with 1.5 months of age being the peak time for detection of IFN β (Thaney et al. 2017) - we found that young non-infected gp120tg- mice had the highest mRNA expression of IFN α , and IFN β across all three brain regions. This expression appeared to decrease with gp120 expression, age, and/or LP-BM5 infection depending on the brain regions. This supports the notion that HIV gp120, presence of virus in the CNS, and aging all could lead to the reduction of innate immunity against HIV infection (Acchioni et al. 2015), allowing the virus to multiply and cause further tissue damage.

It has been reported that the protective effects of IFN β in gp120tg+ mice are in part mediated by the induction of CCL4 (Thaney et al. 2017). However, in our study, the levels of IFN β showed little correlation with CCL4 in any of the brain regions we examined. It is important to note that, in the previous study, cytokine levels were measured in the entire brain hemisphere rather than specific brain regions. Thus, other downstream IFN β -stimulated gene products may be critical in specific brain regions to carry out type I IFN-induced protections.

Our results with CCL2 and CXCL10 revealed that the expression of these two chemokines are mostly gp120-dependent. Particularly for CXCL10, gp120-induced expression of CXCL10 was increased with age and not significantly affected by LP-BM5 treatment (although CXCL10 expression showed a slight decreasing trend with LP-BM5 treatment). This is consistent with a previous study that indicated gp120 could stimulate CXCL10 expression by astrocytes through an IFN γ /STAT1 independent pathway (Asensio et al. 2001). Therefore, CXCL10 could serve as a biomarker to monitor the presence of HIV gp120 viral protein in the CNS and the subsequent development of HAND regardless of systemic immunodeficiency. Supporting this notion, it has been reported that blood levels of CXCL10 could be used to estimate viral loads during early HIV infection (Lee et al. 2015) and as an indication of a more rapid onset of infection (Ploquin et al. 2016). Further, another recent study identified plasma CXCL10 as a biomarker for neurocognitive impairment in women (Burlacu et al. 2019).

In summary, our study was the first step towards examining gp120-induced brain regional difference under immunocompetent vs. immunodeficient conditions. Here, we reported significant brain region-dependent inflammatory responses induced by gp120, which is differentially affected by immune status and the presence of retrovirus in the CNS. Further detailed examination of each HAND-related brain region in conjunction with the systemic immune status is necessary for developing novel targeted treatment for HAND. In addition, further studies should be conducted to explore a broader usage of CXCL10 as a biomarker for HAND.

Acknowledgments The authors would like to thank Dr. Marcus Kaul from the Infectious and Inflammatory Disease Center, Sanford-Burnham Medical Research Institute, La Jolla, CA (later relocated to University of California Riverside, Riverside, CA, USA) for kindly providing the HIV gp120tg mice. We also would like to thank Dr. William Green from the Dartmouth College Geisel School of Medicine, Hanover, NH for providing the original LP-BM5 viral stock. We are very grateful for Dr. WoonYuen Koh from the Department of Mathematics, UNE College of Arts and Science for providing consultation on statistical analysis. We would also like to thank Sanjay Rau from the University of New England College of Osteopathic Medicine for performing selected PCR assays. This work was funded by NIH grants: NIH/NIGMS P20GM103643 (PD Meng) and NIH/NINDS R01S098426 (PI Cao).

References

- Acchioni C, Marsili G, Perrotti E, Remoli AL, Sgarbanti M, Battistini A (2015) Type I IFN—a blunt spear in fighting HIV-1 infection. *Cytokine Growth Factor Rev* 26:143–158. <https://doi.org/10.1016/j.cytogfr.2014.10.004>
- Anthony IC, Ramage SN, Carnie FW, Simmonds P, Bell JE (2005) Influence of HAART on HIV-related CNS disease and neuroinflammation. *J Neuropathol Exp Neurol* 64:529–536. <https://doi.org/10.1093/jnen/64.6.529>
- Anthony IC, Arango JC, Stephens B, Simmonds P, Bell JE (2008) The effects of illicit drugs on the HIV infected brain. *Front Biosci* 13: 1294–1307. <https://doi.org/10.2741/2762>
- Asensio VC et al (2001) Interferon-independent, human immunodeficiency virus type 1 gp120-mediated induction of CXCL10/IP-10 gene expression by astrocytes in vivo and in vitro. *J Virol* 75: 7067–7077. <https://doi.org/10.1128/jvi.75.15.7067-7077.2001>
- Avdoshina V, Fields JA, Castellano P, Dedoni S, Palchik G, Trejo M, Adame A, Rockenstein E, Eugenin E, Masliah E, Mocchielli I (2016) The HIV protein gp120 alters mitochondrial dynamics in neurons. *Neurotox Res* 29:583–593. <https://doi.org/10.1007/s12640-016-9608-6>
- Bell JE (2004) An update on the neuropathology of HIV in the HAART era. *Histopathology* 45:549–559. <https://doi.org/10.1111/j.1365-2559.2004.02004.x>
- Bell JE, Brettle RP, Chiswick A, Simmonds P (1998) HIV encephalitis, proviral load and dementia in drug users and homosexuals with AIDS. Effect of neocortical involvement. *Brain* 121(Pt 11):2043–2052. <https://doi.org/10.1093/brain/121.11.2043>
- Benice TS, Rizk A, Kohama S, Pfankuch T, Raber J (2006) Sex-differences in age-related cognitive decline in C57BL/6J mice associated with increased brain microtubule-associated protein 2 and synaptophysin immunoreactivity. *Neuroscience* 137:413–423. <https://doi.org/10.1016/j.neuroscience.2005.08.029>
- Brabers NACH, Nottet HSLM (2006) Role of the pro-inflammatory cytokines TNF- α and IL-1 β in HIV-associated dementia. *Eur J Clin Invest* 36:447–458. <https://doi.org/10.1111/j.1365-2362.2006.01657.x>
- Bradley H, Hall HI, Wolitski RJ, van Handel M, Stone AE, LaFlam M, Skarbinski J, Higa DH, Prejean J, Frazier EL, Patel R, Huang P, An Q, Song R, Tang T, Valleroy LA (2014) Vital signs: HIV diagnosis, care, and treatment among persons living with HIV—United States, 2011. *MMWR Morb Mortal Wkly Rep* 63:1113–1117
- Burlacu R, Umlauf A, Marcotte TD, Soontornniyomkij B, Diaconu CC, Bulacu-Talnariu A, Temereanca A, Ruta SM, Letendre S, Ene L, Achim CL (2019) Plasma CXCL10 correlates with HAND in HIV-infected women. *Journal of NeuroVirology* 26:23–31. <https://doi.org/10.1007/s13365-019-00785-4>
- Cantres-Rosario YM, Ortiz-Rodríguez SC, Santos-Figueroa AG, Plaud M, Negron K, Cotto B, Langford D, Melendez LM (2019) HIV infection induces extracellular Cathepsin B uptake and damage to neurons. *Sci Rep* 9:8006. <https://doi.org/10.1038/s41598-019-44463-1>
- Cao L, Palmer CD, Malon JT, De Leo JA (2009) Critical role of microglial CD40 in the maintenance of mechanical hypersensitivity in a murine model of neuropathic pain. *Eur J Immunol* 39:3562–3569. <https://doi.org/10.1002/eji.200939657>
- Cao L, Butler MB, Tan L, Dralean KS, Koh WY (2012) Murine immunodeficiency virus-induced peripheral neuropathy and the associated cytokine responses. *J Immunol* 189:3724–3733. <https://doi.org/10.4049/jimmunol.1201313>
- Cary DC, Clements JE, Henderson AJ (2013) RON receptor tyrosine kinase, a negative regulator of inflammation, is decreased during simian immunodeficiency virus-associated central nervous system disease. *J Immunol* 191:4280–4287. <https://doi.org/10.4049/jimmunol.1300797>
- Chauhan N, Siegel G (1997) Age-dependent organotypic expression of microtubule-associated proteins (MAP1, MAP2, and MAP5) in rat brain. *Neurochem Res* 22:713–719. <https://doi.org/10.1023/a:1027306227402>
- Christophi GP, Hudson CA, Panos M, Gruber RC, Massa PT (2009) Modulation of macrophage infiltration and inflammatory activity by the phosphatase SHP-1 in virus-induced demyelinating disease. *J Virol* 83:522–539. <https://doi.org/10.1128/jvi.01210-08>
- Cook WJ, Green KA, Obar JJ, Green WR (2003) Quantitative analysis of LP-BM5 murine leukemia retrovirus RNA using real-time RT-PCR.

- J Virol Methods 108:49–58. [https://doi.org/10.1016/S0166-0934\(02\)00256-2](https://doi.org/10.1016/S0166-0934(02)00256-2)
- Deacon RM, Rawlins JN (2006) T-maze alternation in the rodent. *Nat Protoc* 1:7–12. <https://doi.org/10.1038/nprot.2006.2>
- Dehmelt L, Halpain S (2005) The MAP2/tau family of microtubule-associated proteins. *Genome Biol* 6:204. <https://doi.org/10.1186/gb-2004-6-1-204>
- Deshmane SL, Kremlev S, Amini S, Sawaya BE (2009) Monocyte chemoattractant protein-1 (MCP-1): an overview. *J Interf Cytokine Res* 29:313–326. <https://doi.org/10.1089/jir.2008.0027>
- D'Hooge R, Franck F, Mucke L, De Deyn PP (1999) Age-related behavioural deficits in transgenic mice expressing the HIV-1 coat protein gp120. *Eur J Neurosci* 11:4398–4402. <https://doi.org/10.1046/j.1460-9568.1999.00857.x>
- Di Stefano G, Casoli T, Fattoretti P, Gracciotti N, Solazzi M, Bertoni-Freddari C (2001) Distribution of map2 in hippocampus and cerebellum of young and old rats by quantitative immunohistochemistry. *J Histochem Cytochem* 49:1065–1066. <https://doi.org/10.1177/002215540104900818>
- Dickens AM, Yoo SW, Chin AC, Xu J, Johnson TP, Trout AL, Hauser KF, Haughey NJ (2017) Chronic low-level expression of HIV-1 tat promotes a neurodegenerative phenotype with aging. *Sci Rep* 7:7748. <https://doi.org/10.1038/s41598-017-07570-5>
- Eastwood SL, Weickert CS, Webster MJ, Herman MM, Kleinman JE, Harrison PJ (2006) Synaptophysin protein and mRNA expression in the human hippocampal formation from birth to old age. *Hippocampus* 16:645–654. <https://doi.org/10.1002/hipo.20194>
- Ellis R, Langford D, Masliah E (2007) HIV and antiretroviral therapy in the brain: neuronal injury and repair. *Nat Rev Neurosci* 8:33–44. <https://doi.org/10.1038/nrn2040>
- Fields JA, Serger E, Campos S, Divakaruni AS, Kim C, Smith K, Trejo M, Adame A, Spencer B, Rockenstein E, Murphy AN, Ellis RJ, Letendre S, Grant I, Masliah E (2016) HIV alters neuronal mitochondrial fission/fusion in the brain during HIV-associated neurocognitive disorders. *Neurobiol Dis* 86:154–169. <https://doi.org/10.1016/j.nbd.2015.11.015>
- Force UPST (2019) Screening for HIV infection: US preventive services task force recommendation statement. *JAMA* 321:2326–2336. <https://doi.org/10.1001/jama.2019.6587>
- Giese NA, Giese T, Morse HC (1994) Murine AIDS is an antigen-driven disease: requirements for major histocompatibility complex class II expression and CD4+ T cells. *J Virol* 68:5819–5824
- Gonzalez E, Rovin BH, Sen L, Cooke G, Dhanda R, Mummidi S, Kulkarni H, Bamshad MJ, Telles V, Anderson SA, Walter EA, Stephan KT, Deucher M, Mangano A, Bologna R, Ahuja SS, Dolan MJ, Ahuja SK (2002) HIV-1 infection and AIDS dementia are influenced by a mutant MCP-1 allele linked to increased monocyte infiltration of tissues and MCP-1 levels. *Proc Natl Acad Sci U S A* 99:13795–13800. <https://doi.org/10.1073/pnas.202357499>
- Green KA, Cook WJ, Green WR (2013) Myeloid-derived suppressor cells in murine retrovirus-induced AIDS inhibit T- and B-cell responses *in vitro* that are used to define the immunodeficiency. *J Virol* 87:2058–2071. <https://doi.org/10.1128/jvi.01547-12>
- Guha D, Wagner MCE, Ayyavoo V (2018) Human immunodeficiency virus type 1 (HIV-1)-mediated neuroinflammation dysregulates neurogranin and induces synaptodendritic injury. *J Neuroinflammation* 15:126. <https://doi.org/10.1186/s12974-018-1160-2>
- Hartley JW, Fredrickson TN, Yetter RA, Makino M, Morse HC 3rd (1989) Retrovirus-induced murine acquired immunodeficiency syndrome: natural history of infection and differing susceptibility of inbred mouse strains. *J Virol* 63:1223–1231
- Haughey NJ, Mattson MP (2002) Calcium Dysregulation and neuronal apoptosis by the HIV-1 proteins tat and gp120. *JAIDS journal of acquired immune deficiency syndromes* 31:S55–S61
- Hauser KF, Knapp PE (2014) Interactions of HIV and drugs of abuse: the importance of glia, neural progenitors, and host genetic factors. *Int Rev Neurobiol* 118:231–313. <https://doi.org/10.1016/B978-0-12-801284-0.00009-9>
- Henderson LJ, Johnson TP, Smith BR, Reoma LB, Santamaria UA, Bachani M, Demarino C, Barclay RA, Snow J, Sacktor N, McArthur J, Letendre S, Steiner J, Kashanchi F, Nath A (2019) Presence of tat and transactivation response element in spinal fluid despite antiretroviral therapy. *AIDS* 33(Suppl 2):S145–S157. <https://doi.org/10.1097/QAD.0000000000002268>
- Huang M, Simard C, Jolicoeur P (1992) Susceptibility of inbred strains of mice to murine AIDS (MAIDS) correlates with target cell expansion and high expression of defective MAIDS virus. *J Virol* 66:2398–2406
- Janda E, Visalli V, Colica C, Aprigliano S, Musolino V, Vadalà N, Muscoli C, Sacco I, Iannone M, Rotiroli D, Spedding M, Mollace V (2011) The protective effect of tianeptine on Gp120-induced apoptosis in astroglial cells: role of GS and NOS, and NF-κB suppression. *Br J Pharmacol* 164:1590–1599. <https://doi.org/10.1111/j.1476-5381.2010.01172.x>
- Janssen MA, Meulenbroek O, Steens SC, Goraj B, Bosch M, Koopmans PP, Kessels RP (2015) Cognitive functioning, wellbeing and brain correlates in HIV-1 infected patients on long-term combination antiretroviral therapy. *AIDS* 29:2139–2148. <https://doi.org/10.1097/QAD.0000000000000824>
- Kalcheva N, Albala J, O'Guin K, Rubino H, Garner C, Shafit-Zagardo B (1995) Genomic structure of human microtubule-associated protein 2 (MAP-2) and characterization of additional MAP-2 isoforms. *Proc Natl Acad Sci U S A* 92:10894–10898. <https://doi.org/10.1073/pnas.92.24.10894>
- Kallianpur KJ, Gerschenson M, Mitchell BI, LiButti DE, Umaki TM, Ndhlovu LC, Nakamoto BK, Chow DC, Shikuma CM (2016) Oxidative mitochondrial DNA damage in peripheral blood mononuclear cells is associated with reduced volumes of hippocampus and subcortical gray matter in chronically HIV-infected patients. *Mitochondrion* 28:8–15. <https://doi.org/10.1016/j.mito.2016.02.006>
- Kelder W, McArthur JC, Nance-Sproson T, McClemon D, Griffin DE (1998) β-Chemokines MCP-1 and RANTES are selectively increased in cerebrospinal fluid of patients with human immunodeficiency virus-associated dementia. *Ann Neurol* 44:831–835. <https://doi.org/10.1002/ana.410440521>
- Kolb SA, Sporer B, Lahrtz F, Koedel U, Pfister H-W, Fontana A (1999) Identification of a T cell chemotactic factor in the cerebrospinal fluid of HIV-1-infected individuals as interferon-γ inducible protein 10. *J Neuroimmunol* 93:172–181. [https://doi.org/10.1016/S0165-5728\(98\)00223-9](https://doi.org/10.1016/S0165-5728(98)00223-9)
- Krucker T, Toggas SM, Mucke L, Siggins GR (1998) Transgenic mice with cerebral expression of human immunodeficiency virus type-1 coat protein gp120 show divergent changes in short- and long-term potentiation in CA1 hippocampus. *Neuroscience* 83:691–700. [https://doi.org/10.1016/S0306-4522\(97\)00413-2](https://doi.org/10.1016/S0306-4522(97)00413-2)
- Kundu K, Dutta K, Nazmi A, Basu A (2013) Japanese encephalitis virus infection modulates the expression of suppressors of cytokine signaling (SOCS) in macrophages: Implications for the hosts' innate immune response. *Cell Immunol* 285:100–110. <https://doi.org/10.1016/j.cellimm.2013.09.005>
- Lalonde R (2002) The neurobiological basis of spontaneous alternation. *Neurosci Biobehav Rev* 26:91–104. [https://doi.org/10.1016/s0149-7634\(01\)00041-0](https://doi.org/10.1016/s0149-7634(01)00041-0)
- Lee I, Kesner RP (2003) Time-dependent relationship between the dorsal hippocampus and the prefrontal cortex in spatial memory. *J Neurosci* 23:1517–1523. <https://doi.org/10.1523/jneurosci.23-04-01517.2003>
- Lee S, Chung Y-S, Yoon C-H, Shin Y, Kim S, Choi B-S, Kim SS (2015) Interferon-inducible protein 10 (IP-10) is associated with viremia of

- early HIV-1 infection in Korean patients. *J Med Virol* 87:782–789. <https://doi.org/10.1002/jmv.24026>
- Letendre SL, Ellis RJ, Everall I, Ances B, Bharti A, McCutchan JA (2009) Neurologic complications of HIV disease and their treatment. *Top HIV Med* 17:46–56
- Li W, Green WR (2006) The role of CD4 T cells in the pathogenesis of murine AIDS. *J Virol* 80:5777–5789. <https://doi.org/10.1128/jvi.02711-05>
- Maartens G, Celum C, Lewin SR (2014) HIV infection: epidemiology, pathogenesis, treatment, and prevention. *Lancet* 384:258–271. [https://doi.org/10.1016/S0140-6736\(14\)60164-1](https://doi.org/10.1016/S0140-6736(14)60164-1)
- Masliah E, Ellis RJ, Mallory M, Heaton RK, Marcotte TD, Nelson JA, Grant I, Atkinson JH, Wiley CA, Achim CL, JA MC, The HNRC Group (1997) Dendritic injury is a pathological substrate for human immunodeficiency virus-related cognitive disorders. HNRC group. The HIV Neurobehavioral Research Center. *Ann Neurol* 42:963–972. <https://doi.org/10.1002/ana.410420618>
- Maung R et al (2014) CCR5 knockout prevents neuronal injury and behavioral impairment induced in a transgenic mouse model by a CXCR4-using HIV-1 glycoprotein 120. *J Immunol* 193:1895–1910. <https://doi.org/10.4049/jimmunol.1302915>
- McArthur JC, Steiner J, Sacktor N, Nath A (2010) Human immunodeficiency virus-associated neurocognitive disorders: Mind the gap. *Ann Neurol* 67:699–714. <https://doi.org/10.1002/ana.22053>
- McLane VD, Cao L, Willis CL (2014) Morphine increases hippocampal viral load and suppresses frontal lobe CCL5 expression in the LP-BM5 AIDS model. *J Neuroimmunol* 269:44–51. <https://doi.org/10.1016/j.jneuroim.2014.02.010>
- McLane VD, Kumar S, Leeming R, Rau S, Willis CL, Cao L (2018) Morphine-potentiated cognitive deficits correlate to suppressed hippocampal iNOS RNA expression and an absent type I interferon response in LP-BM5 murine AIDS. *J Neuroimmunol* 319:117–129. <https://doi.org/10.1016/j.jneuroim.2018.02.017>
- McLaurin KA, Li H, Booze RM, Mactutus CF (2019) Disruption of Timing: NeuroHIV Progression in the Post-cART Era. *Sci Rep* 9: 827. <https://doi.org/10.1038/s41598-018-36822-1>
- Moore DJ et al (2006) Cortical and subcortical neurodegeneration is associated with HIV neurocognitive impairment. *AIDS* 20:879–887. <https://doi.org/10.1097/01.aids.0000218552.69834.00>
- Mutnal MB, Schachtele SJ, Hu S, Lokensgard JR (2013) T-cell reconstitution during murine acquired immunodeficiency syndrome (MAIDS) produces neuroinflammation and mortality in animals harboring opportunistic viral brain infection. *J Neuroinflammation* 10:863. <https://doi.org/10.1186/1742-2094-10-98>
- Nasi M, de Biasi S, Gibellini L, Bianchini E, Pecorini S, Bacca V, Guaraldi G, Mussini C, Pinti M, Cossarizza A (2017) Ageing and inflammation in patients with HIV infection. *Clin Exp Immunol* 187:44–52. <https://doi.org/10.1111/cei.12814>
- Piggott DA, Bandeen-Roche K, Mehta SH, Brown TT, Yang H, Walston JD, Leng SX, Kirk GD (2020) Frailty transitions, inflammation and mortality among persons aging with HIV infection and injection drug use. *AIDS* 34:1217–1225. <https://doi.org/10.1097/QAD.0000000000002527>
- Ploquin MJ, Madec Y, Casrouge A, Huot N, Passaes C, Lécroux C, Essat A, Boufassa F, Jacquelin B, Jochems SP, Petitjean G, Angin M, Gärtner K, Garcia-Tellez T, Noël N, Booiman T, Boeser-Nunnink BD, Roques P, Saez-Cirion A, Vaslin B, Dereudre-Bosquet N, Barré-Sinoussi F, Ghislain M, Rouzioux C, Lambotte O, Albert ML, Goujard C, Kootstra N, Meyer L, Müller-Trutwin MC (2016) Elevated basal pre-infection CXCL10 in plasma and in the small intestine after infection are associated with more rapid HIV/SIV disease onset. *PLoS Pathog* 12:e1005774. <https://doi.org/10.1371/journal.ppat.1005774>
- Ronaldson PT, Bendayan R (2006) HIV-1 viral envelope glycoprotein gp120 triggers an inflammatory response in cultured rat astrocytes and regulates the functional expression of P-glycoprotein. *Mol Pharmacol* 70:1087–1098. <https://doi.org/10.1124/mol.106.025973>
- Saylor D, Dickens AM, Sacktor N, Haughey N, Slusher B, Pletnikov M, Mankowski JL, Brown A, Volsky DJ, McArthur JC (2016) HIV-associated neurocognitive disorder—pathogenesis and prospects for treatment. *Nat Rev Neurol* 12:234–248. <https://doi.org/10.1038/nrneuro.2016.27>
- Sivro A, Su RC, Plummer FA, Ball TB (2014) Interferon responses in HIV infection: from protection to disease. *AIDS Rev* 16:43–51
- Spudich S, Robertson KR, Bosch RJ, Gandhi RT, Cyktor JC, Mar H, Macatangay BJ, Lalama CM, Rinaldo C, Collier AC, Godfrey C, Eron JJ, McMahon D, Jacobs JL, Koontz D, Hogg E, Vecchio A, Mellors JW (2019) Persistent HIV-infected cells in cerebrospinal fluid are associated with poorer neurocognitive performance. *J Clin Invest* 129:3339–3346. <https://doi.org/10.1172/JCI127413>
- Thaney VE, O'Neill AM, Hoefer MM, Maung R, Sanchez AB, Kaul M (2017) IFN β Protects Neurons from Damage in a Murine Model of HIV-1 Associated Brain Injury. *Sci Rep* 7:46514. <https://doi.org/10.1038/srep46514> <https://www.nature.com/articles/srep46514#supplementary-information>
- Thaney VE, Sanchez AB, Fields JA, Minassian A, Young JW, Maung R, Kaul M (2018) Transgenic mice expressing HIV-1 envelope protein gp120 in the brain as an animal model in neuroAIDS research. *J Neurovirol* 24:156–167. <https://doi.org/10.1007/s13365-017-0584-2>
- Toggas SM, Masliah E, Rockenstein EM, Rail GF, Abraham CR, Mucke L (1994) Central nervous system damage produced by expression of the HIV-1 coat protein gp120 in transgenic mice. *Nature* 367:188–193. <https://doi.org/10.1038/367188a0>
- Watanabe D et al (2010) Sustained high levels of serum interferon- γ during HIV-1 infection: a specific trend different from other cytokines. *Viral Immunol* 23:619–625. <https://doi.org/10.1089/vim.2010.0065>
- Watkins CC, Treisman GJ (2015) Cognitive impairment in patients with AIDS - prevalence and severity. *HIV AIDS (Auckl)* 7:35–47. <https://doi.org/10.2147/HIV.S39665>
- Wei J, Carroll RJ, Harden KK, Wu G (2012) Comparisons of treatment means when factors do not interact in two-factorial studies. *Amino Acids* 42:2031–2035. <https://doi.org/10.1007/s00726-011-0924-0>
- Weisberg DF et al (2015) Long-term prescription of opioids and/or benzodiazepines and mortality among HIV-infected and uninfected patients. *J Acquir Immune Defic Syndr* 69:223–233. <https://doi.org/10.1097/QAI.0000000000000591>
- Williams D, Anastos K, Morgello S, Berman J (2014) JAM-A and ALCAM are therapeutic targets to inhibit diapedesis across the BBB of CD14+ CD16+ monocytes in HIV-infected individuals. *J Leukoc Biol* 97:401–412. <https://doi.org/10.1189/jlb.5A0714-347R>
- Yeung MC, Pulliam L, Lau AS (1995) The HIV envelope protein gp120 is toxic to human brain-cell cultures through the induction of interleukin-6 and tumor necrosis factor- α . *AIDS* 9:137–143
- Yu YF, Zhai F, Dai CF, Hu JJ (2011) The relationship between age-related hearing loss and synaptic changes in the hippocampus of C57BL/6J mice. *Exp Gerontol* 46:716–722. <https://doi.org/10.1016/j.exger.2011.04.007>
- Zhu Q et al (2015) Target of HIV-1 envelope glycoprotein gp120-induced hippocampal neuron damage: role of voltage-gated K(+) channel Kv2.1. *Viral Immunol* 28:495–503. <https://doi.org/10.1089/vim.2015.0020>